Effect of Particle-Phonon Coupling on Pairing Correlations in Nuclei

J. Terasaki
Department of Physics, University of Milan, Via Celoria 16, I-20133 Milan, Italy;
and INFN Sezione di Milano, Via Celoria 16, I-20133 Milan, Italy
E-mail: terasaki@mi.infn.it

F. Barranco
Escuela Superior de Ingenieros Industriales, Universidad de Sevilla,
Camino de los Descrubimientos, 41092 Sevilla, Spain
E-mail: barranco@cica.es

P.F. Bortignon
Department of Physics, University of Milan, Via Celoria 16, I-20133 Milan, Italy
E-mail: bortignon@mi.infn.it

R. A. Broglia
Department of Physics, University of Milan, Via Celoria 16, I-20133 Milan, Italy;
INFN Sezione di Milano, Via Celoria 16, I-20133 Milan, Italy;
and The Niels Bohr Institute, University of Copenhagen, D-2100 Copenhagen, Denmark
E-mail: broglia@mi.infn.it

and

E. Vigezzi
INFN Sezione di Milano, Via Celoria 16, I-20133 Milan, Italy
E-mail: vigezzi@mi.infn.it

September 17, 2001

Abstract

The influence of particle-phonon coupling on pairing correlations in nuclei is studied by solving the Dyson equation including the anomalous (pairing) Green function. We develop the formalism for solving the equation with the minimum of approximations. The solution of the Dyson equation is compared with the diagonalization of particle-phonon coupled Hamiltonian in a small space. This comparison reveals that the effect of many-phonon states is incorporated in the Dyson equation. We calculate the pairing gap of the neutron in ^{120}Sn. We compare analytically the present method with a simpler treatment based on Bloch-Horowitz perturbation theory.

1 Introduction

The study of the nature of pairing correlations is one of the most fundamental problems in nuclear physics. These correlations have been introduced in the study of nuclear structure in analogy with the case of metals [1] and since then played an important role in the understanding of many aspects of nuclear behaviour, because they affect static and dynamic properties of atomic nuclei, their structure as well as their reactions. One can quote, for example, the systematic staggering of the odd-even mass difference (section 2-1 in [2]), the reduction of the moment of inertia of collective rotational bands as compared to the rigid-body value (section 4-3 in [3]), the enhancement of the two-particle transfer reactions to specific final states [4], the appearance of signals in both one-particle pick-up and stripping reactions for the same single-particle orbit near the Fermi level (section 5-3 in [3]), the lifetimes of α decay in the heavy mass region [5] and so on. Influence of the pairing gap can be also found in the spectra of deformed nuclei.[1] [1] Namely, the spacing of the low-lying non-collective excited states (band heads) in odd nuclei is reduced in average due to the pairing gap [6]. Two-quasiparticle states are of relatively high energy in heavy even-even nuclei, because breaking the pair costs energy. The feature analogous to the latter can be seen also in odd nuclei (sections 5-2 and 5-3 in [3]). The interplay between the pairing and the other degrees of freedom also plays an important role. For example, pairing correlations are suppressed by rotation [7, 8].

Since pairing correlations play such an important role, it is crucial to ask what is their origin.

Pairing correlations in finite nuclei have mostly been studied in mean field theory through BCS and Hartree-Fock-Bogoliubov (HFB) calculations, making use of phenomenological interactions, the monopole pairing interaction having probably been the most often used (e. g. [9]). The list of the interactions may include the quadrupole pairing interaction (used for improving the monopole pairing interaction, see e. g. [10] for rotation and [11] for the pairing vibration.), the surface-delta interaction e. g. [12], [13] and [14], density-dependent zero-range pairing forces [15], the Gogny force, [16] and [17], and so on.

Recently, several studies have been devoted to pairing in nuclei near the drip line, for which it is crucial that the pairing force treats correctly the interplay between the discrete and continuum unperturbed single-particle levels correctly: that is, summation of the unbound components of many-body wavefunction caused by the interplay must be canceled out [18],[19].

The connections of pairing correlations in finite nuclei with the bare interactions, that is, on interactions which reproduce the properties of scattering of free nucleons, have been very scarce in finite nuclei (for a few exceptions, cf. [20],[21] and [22]). On the other hand, this represents an important line of research in nuclear matter ([23]–[27] and references therein) and in its applications to nuclear astrophysics, where for example pairing plays a very important role in the cooling of the neutron stars by neutrino emission (e. g. [28]). Also much studied have been the effects of medium polarization on pairing correlations. In terms of field theory this effect is given by bubble diagrams of the particle-hole excitations [29]–[34].

[1] The influence can be recognized in average for low-lying levels. Evidence of the correlations in each level is not always easy to find due to state dependence of the pairing gap.

In the limit of infinite number of the bubbles, one can think of an interaction between nucleons mediated by the exchange of phonons (phonon-induced interaction). In this idea the coupling, or vertex, between particle[2] [2] and phonon is crucially important, and the influences of this coupling on many properties of phonons as well as of particles have been investigated intensively in finite nuclei, although not its effect on pairing correlations. In particular, the coupling with low-lying surface vibrations renormalizes the single-particle motion in an essential way, shifting the energy of the levels and changing the level density and the effective mass around the Fermi surface, and producing a significant breaking of the single-particle strength for the levels lying far from the Fermi surface [30],[35].

A formulation which can properly investigate the effect of the particle-phonon coupling on pairing correlations in nuclei was already proposed in 1960's by Belyaev et al. [36, 37, 38] and Migdal et al. [39, 40] on the basis of field theory. The key point of the method is to introduce anomalous (pairing) Green functions in addition to normal Green functions. In condensed matter physics this formulation was introduced by Gor'kov [41] and Nambu [42], and the original dynamical equation was rearranged with approximations characteristic in the metal and is known as Eliashberg equation [43] or Gor'kov equation, which was shown to be powerful in the calculation of the tunneling probability. A relatively recent review is given by [44]. The application of the particle-phonon coupling to pairing problems in finite nuclei has been, however, surprisingly rare. Recently Barranco et al. solved BCS equation with the phonon-induced interaction obtained according to Bloch-Horowitz perturbation [45]. They have also shown the crucial importance of this coupling for the stability of the halo nucleus ^{11}Li [46]. Avdeenkov and Kamerdzhiev [47] solve the Dyson equation in the linear approximation. (See also [48].) Keeping in mind the historical background described above, we investigate in this paper the effect of the phonon-induced interaction on nuclear pairing correlations.

We solve the Dyson equation consisting of the one-body as well as anomalous Green functions for particle-phonon coupled systems and calculate the pairing gaps. The phonon is treated as an independent degree of freedom. In nuclei, this is a technique to treat complicated diagrams of interaction nonperturbatively. Introduction of the anomalous Green function can be understood also as this kind of technique. It is emphasized that in the field-theoretical approach it is possible to include effects beyond the mean field as well as the mean pair-field approximation, which manifest themself in the fragmentation of the single-particle strength. After making a choice of proper self-energy diagrams, we solve Dyson equation with the minimum of approximations, being careful not to suppress the effects beyond BCS. Thus the most significant point of this study is that we investigate the pairing correlation without assuming a priori that the single-particle or quasiparticle picture is good. In addition a class of diagrams is included nonperturbatively in the calculation. We shall pay attention also to relation between this approach and diagonalization of particle-phonon coupled Hamiltonian in the many-body plus phonon space.

Finally let us mention two more groups concerning the Dyson equation in nuclear-structure. One of them is Müther and Dickhoff et al. They developed an approx-

[2]This terminology is used in different ways depending on the context. One is a single-particle sitting on a level above the Fermi level, and another is simply single-particle or nucleon. In this paper we use the terminology mainly in the latter sense.

imate way to solve Dyson equation [49] (without the anomalous Green function) and applied their method to doubly-magic nuclei [50]–[54] with a nucleon-nucleon interaction, emphasizing fragmentation of the single-particle strength. An application was made also to nuclear matter [55]. Another group which we note is Waroquier et al. They proposed another way to approximate a solution of Dyson equation and applied it to some nuclei [56, 57, 58]. They performed calculation also for an open-shell nucleus [59] using a formulation which includes a concept of the pairing gap, however, the gap was not discussed in their paper. This group uses both nucleon-nucleon interaction and particle-phonon coupling. A comparison was made of the two methods of the groups in [60].

This paper is organized as follows: In section 2 we discuss the formulation and describe our way to solve the Dyson equation. We also consider the relation between diagrams with and without the anomalous Green functions. In the next section detailed comparisons are made between the solution of Dyson equation and the diagonalization of the particle-phonon coupled Hamiltonian. Section 4 shows results of the calculation of the neutrons in ^{120}Sn using Dyson equation. We discuss the spectral functions, pairing gaps, the single-particle energy shifts and the pairing energy. BCS approximation is discussed briefly in section 5. The last section is devoted to a summary. The equations used in this paper are derived thoroughly in appendices. Appendix A is for the derivation of the diagram rule. The self-energy used in the calculation is derived in Appendix B. The next appendix is about the general form of the particle Green functions, and some useful relations are derived. Appendix D treats equations for calculating the poles and the residues. The equations of the total energy and the pairing gaps are derived in Appendices E and F, respectively.

2 Formulation

The core of this study is the Dyson equation

$$G_\mu^{-1}(\omega) = {G_\mu^0}^{-1}(\omega) - \Sigma_\mu(\omega) \ , \tag{1}$$

where each term is a 2×2 matrix, i. e.,

$$G_\mu(\omega) = \begin{pmatrix} G_\mu^{11}(\omega) & G_\mu^{12}(\omega) \\ G_\mu^{21}(\omega) & G_\mu^{22}(\omega) \end{pmatrix} \ , \tag{2}$$

$$G_\mu^0(\omega) = \begin{pmatrix} {G_\mu^0}^{11}(\omega) & {G_\mu^0}^{12}(\omega) \\ {G_\mu^0}^{21}(\omega) & {G_\mu^0}^{22}(\omega) \end{pmatrix} \ , \tag{3}$$

$$\Sigma_\mu(\omega) = \begin{pmatrix} \Sigma_\mu^{11}(\omega) & \Sigma_\mu^{12}(\omega) \\ \Sigma_\mu^{21}(\omega) & \Sigma_\mu^{22}(\omega) \end{pmatrix} \ , \tag{4}$$

with ω being an energy variable. $G_\mu(\omega)$ is a perturbed nucleon Green function obtained by solving the equation. μ denotes the spherical good quantum numbers $(nlj)_\mu$ of a single-particle orbit throughout this paper except for Appendix A which treats the most general case. We assume that the system considered has spherical

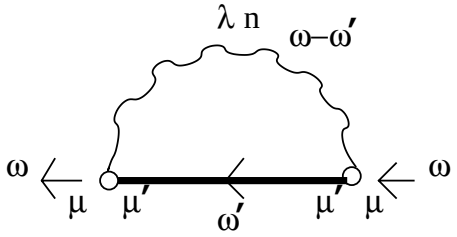

Figure 1. The self-energy. ω and ω' denote the energy variable. λ stands for the multipolarity of phonon, and μ and μ' are the single-particle indices.

symmetry. The off-diagonal elements of $G_\mu(\omega)$ are anomalous Green functions. $G^0_\mu(\omega)$ is an unperturbed nucleon Green function

$$\frac{1}{\hbar}G_\mu^{0\,11}(\omega) = \frac{e^{i\eta\omega}}{\omega - (\varepsilon^0_\mu - \varepsilon_F) + i\eta_\mu} \ , \tag{5}$$

$$\frac{1}{\hbar}G_\mu^{0\,12}(\omega) = \frac{1}{\hbar}G_\mu^{0\,21}(\omega) = 0 \ , \tag{6}$$

$$\frac{1}{\hbar}G_\mu^{0\,22}(\omega) = \frac{e^{-i\eta\omega}}{\omega + (\varepsilon^0_\mu - \varepsilon_F) - i\eta_\mu} \ , \tag{7}$$

where ε^0_μ denotes an unperturbed single-particle energy, and ε_F is Fermi level. η_μ is a parameter as

$$\eta_\mu = \begin{cases} -\eta \ , & \varepsilon^0_\mu < \varepsilon_F \\ \eta \ , & \varepsilon^0_\mu > \varepsilon_F \end{cases} \tag{8}$$

where η is a real positive parameter. In this study we consider a self-energy $\Sigma_\mu(\omega)$ given by the diagram in Fig. 1.

The wavy line in Fig. 1 denotes an unperturbed phonon Green function

$$\frac{i}{\hbar}D^0_{\lambda n}(\omega - \omega') = \frac{i}{\omega - \omega' - \hbar\Omega_{\lambda n} + i\eta_D} + \frac{i}{-\omega + \omega' - \hbar\Omega_{\lambda n} + i\eta_D} \ , \tag{9}$$

where $\hbar\Omega_{\lambda n}$ is the phonon energy with the multipolarity λ and is uniquely specified by another label n, if many modes have the same λ. η_D stands for a real positive parameter. The thick line indicates the perturbed nucleon Green function $\frac{1}{\hbar}G_{\mu'}(\omega')$. The small open circle is an unperturbed vertex of the phonon and the nucleon:

$$(-)^{j_\mu + j_{\mu'}}\sqrt{\frac{\hbar}{2\Omega_{\lambda n}B_{\lambda n}}}\langle\mu||R_0\frac{dU}{dr}Y_\lambda||\mu'\rangle \ , \tag{10}$$

$B_{\lambda n}$ is the inertia parameter of the phonon. R_0 and $U(r)$ are a nuclear radius and a nuclear potential, respectively. From the diagram we obtain the equation of the self-energy

$$\begin{aligned} \hbar\Sigma_\mu(\omega) \ &= \ \int_{-\infty}^{\infty}\frac{d\omega'}{2\pi}\sum_{\mu'}\tau_3\frac{1}{\hbar}G_{\mu'}(\omega')\tau_3\sum_{\lambda n}\frac{\hbar}{2\Omega_{\lambda n}B_{\lambda n}}\frac{1}{2j_\mu+1} \\ &\quad\times\left|\langle\mu||R_0\frac{dU}{dr}Y_\lambda||\mu'\rangle\right|^2\frac{i}{\hbar}D^0_{\lambda n}(\omega-\omega') \ , \end{aligned} \tag{11}$$

where $\tau_3 = \begin{pmatrix} 1 & 0 \\ 0 & -1 \end{pmatrix}$. The derivation of the diagram rule is given in Appendix A, and the self-energy in a spherical nucleus is derived in Appendix B.

For solving Eq. (1) we put

$$\frac{1}{\hbar}G_\mu^{11}(\omega) = \sum_a \left(\frac{R_{\mu a}^{11}(\omega_{G+}^{\mu a})}{\omega - \omega_{G+}^{\mu a}} + \frac{R_{\mu a}^{11}(-\omega_{G+}^{\mu a})}{\omega + \omega_{G+}^{\mu a}} \right) e^{i\omega\eta} \ , \tag{12}$$

$$\frac{1}{\hbar}G_\mu^{12}(\omega) = \sum_a \left(\frac{R_{\mu a}^{12}(\omega_{G+}^{\mu a})}{\omega - \omega_{G+}^{\mu a}} + \frac{R_{\mu a}^{12}(-\omega_{G+}^{\mu a})}{\omega + \omega_{G+}^{\mu a}} \right) \ . \tag{13}$$

Assuming the time-reversal invariance of the ground state, we can put

$$\frac{1}{\hbar}G_\mu^{22}(\omega) = \sum_a \left(\frac{R_{\mu a}^{11}(-\omega_{G+}^{\mu a})}{\omega - \omega_{G+}^{\mu a}} + \frac{R_{\mu a}^{11}(\omega_{G+}^{\mu a})}{\omega + \omega_{G+}^{\mu a}} \right) e^{-i\omega\eta} \ , \tag{14}$$

$$\frac{1}{\hbar}G_\mu^{21}(\omega) = \sum_a \left(\frac{R_{\mu a}^{12\,*}(\omega_{G+}^{\mu a})}{\omega - \omega_{G+}^{\mu a}} + \frac{R_{\mu a}^{12\,*}(-\omega_{G+}^{\mu a})}{\omega + \omega_{G+}^{\mu a}} \right) \ , \tag{15}$$

where $\omega_{G+}^{\mu a}$ denotes a pole of the nucleon Green function ($\mathrm{Re}\,\omega_{G+}^{\mu a} > 0$). a is a label to distinguish poles associated with μ. $R_{\mu a}^{11}(\pm\omega_{G+}^{\mu a})$ are residues of $G_\mu^{11}(\omega)/\hbar$ at the poles $\pm\omega_{G+}^{\mu a}$. Eqs. (12)–(15) are explained in detail in Appendix C. Inserting the above equations to Eq. (11) we obtain

$$\begin{aligned} \hbar\Sigma_\mu^{11}(\omega) &= \sum_{\mu' a}\sum_{\lambda n} \frac{\hbar}{2\Omega_{\lambda n}B_{\lambda n}} \left| \langle \mu || R_0 \frac{dU}{dr} Y_\lambda || \mu' \rangle \right|^2 \frac{1}{2j_\mu + 1} \\ &\quad \times \left\{ \frac{R_{\mu' a}^{11}(-\omega_{G+}^{\mu' a})}{\omega + \omega_{G+}^{\mu' a} + \hbar\Omega_{\lambda n} - i\eta_D} + \frac{R_{\mu' a}^{11}(\omega_{G+}^{\mu' a})}{\omega - \omega_{G+}^{\mu' a} - \hbar\Omega_{\lambda n} + i\eta_D} \right\} \ , \end{aligned} \tag{16}$$

$$\begin{aligned} \hbar\Sigma_\mu^{12}(\omega) &= \sum_{\mu' a}\sum_{\lambda n} \frac{\hbar}{2\Omega_{\lambda n}B_{\lambda n}} \left| \langle \mu || R_0 \frac{dU}{dr} Y_\lambda || \mu' \rangle \right|^2 \frac{-1}{2j_\mu + 1} \\ &\quad \times \left\{ \frac{R_{\mu' a}^{12}(-\omega_{G+}^{\mu' a})}{\omega + \omega_{G+}^{\mu' a} + \hbar\Omega_{\lambda n} - i\eta_D} + \frac{R_{\mu' a}^{12}(\omega_{G+}^{\mu' a})}{\omega - \omega_{G+}^{\mu' a} - \hbar\Omega_{\lambda n} + i\eta_D} \right\} \ . \end{aligned} \tag{17}$$

$\Sigma_\mu^{22}(\omega)$ and $\Sigma_\mu^{21}(\omega)$ can be obtained in the same way. (If $R_{\mu a}^{12}(\pm\omega_{G+}^{\mu a})$'s are real, then $\Sigma_\mu^{12}(\omega) = \Sigma_\mu^{12}(-\omega)$.)

Keeping the idea that stationary states are treated, we calculate $\omega_{G+}^{\mu a}$ and $R_{\mu a}^{11}(\pm\omega_{G+}^{\mu a})$ etc. in the following way. First $\pm\mathrm{Re}\,\omega_{G+}^{\mu a}$ are determined by searching for the points, numerically on the real ω axis, satisfying

$$\det \overline{G}_\mu^{-1}(\pm\mathrm{Re}\,\omega_{G+}^{\mu a}) = 0 \ , \tag{18}$$

where

$$\hbar\overline{G}_\mu^{-1}(\omega) = \begin{pmatrix} \omega - \tilde{\varepsilon}_\mu^0 - \mathrm{Re}\,\hbar\Sigma_\mu^{11}(\omega) & -\hbar\Sigma_\mu^{12}(\omega) \\ -\hbar\Sigma_\mu^{21}(\omega) & \omega + \tilde{\varepsilon}_\mu^0 - \mathrm{Re}\,\hbar\Sigma_\mu^{22}(\omega) \end{pmatrix} \ , \tag{19}$$

with $\tilde{\varepsilon}_\mu^0 = \varepsilon_\mu^0 - \varepsilon_F$. The above equation is the same as $\hbar G_\mu^{-1}(\omega)$ except for the non-hermitian component of the diagonal elements eliminated. We identify the residue of $\overline{G}_\mu^{11}(\omega)/\hbar$ with that of $G_\mu^{11}(\omega)/\hbar$:

$$R_{\mu a}^{11}(\pm\omega_{G+}^{\mu a}) = \left. \frac{\omega + \tilde{\varepsilon}_\mu^0 - \hbar\,\mathrm{Re}\,\Sigma_\mu^{22}(\omega)}{\frac{d}{d\omega}\hbar^2 \det \overline{G}_\mu^{-1}(\omega)} \right|_{\omega = \pm\mathrm{Re}\,\omega_{G+}^{\mu a}} \ , \tag{20}$$

where the derivative is taken on the real axis. For the pairing part the residue is calculated

$$R^{12}_{\mu a}(\omega^{\mu a}_{G+}) = \left. \frac{\Sigma^{12}_{\mu}(\omega)}{\hbar \frac{d}{d\omega} \det \overline{G}^{-1}_{\mu}(\omega)} \right|_{\omega = \mathrm{Re}\, \omega^{\mu a}_{G+}} . \tag{21}$$

The imaginary part of the pole may be approximated by

$$\mathrm{Im}\, \omega^{\mu a}_{G+} \simeq \mathrm{Im}\, \frac{\hbar}{G^{11}_{\mu}(\mathrm{Re}\, \omega^{\mu a}_{G+})} R^{11}_{\mu a}(\omega^{\mu a}_{G+}) \ , \tag{22}$$

or one can set Im $\omega^{\mu a}_{G+}$ equal to a small constant. In section 4 the latter method is used. Eqs. (20)–(22) are an extension of the argument in the sections 3.4 and 4.3.6 in [35], and are discussed in Appendix D.

Eq. (1) can be solved by iteration using the BCS Green function (section 7-2 in [43]) as an initial guess of a solution:

$$\frac{1}{\hbar} G^{\mathrm{B}11}_{\mu}(\omega) = \left(\frac{v^2_{\mu}}{\omega + \mathcal{E}_{\mu} - i\eta} + \frac{u^2_{\mu}}{\omega - \mathcal{E}_{\mu} + i\eta} \right) e^{i\eta\omega} \ , \tag{23}$$

$$\frac{1}{\hbar} G^{\mathrm{B}22}_{\mu}(\omega) = \left(\frac{u^2_{\mu}}{\omega + \mathcal{E}_{\mu} - i\eta} + \frac{v^2_{\mu}}{\omega - \mathcal{E}_{\mu} + i\eta} \right) e^{-i\eta\omega} \ , \tag{24}$$

$$\frac{1}{\hbar} G^{\mathrm{B}12}_{\mu}(\omega) = \frac{-u_{\mu}v_{\mu}}{\omega + \mathcal{E}_{\mu} - i\eta} + \frac{u_{\mu}v_{\mu}}{\omega - \mathcal{E}_{\mu} + i\eta} \ , \tag{25}$$

where $\mathcal{E}_{\mu} = \sqrt{(\varepsilon^0_{\mu} - \varepsilon_F)^2 + \Delta^2}$, u_{μ} and v_{μ} being the occupation factors of BCS theory. Δ is a parameter. The BCS Green function is inserted to Eqs. (16) and (17), i.e.

$$\mathcal{E}_{\mu} \to \mathrm{Re}\, \omega^{\mu}_{G+} \ , \tag{26}$$

$$-\eta \to \mathrm{Im}\, \omega^{\mu}_{G+} \ , \tag{27}$$

$$v^2_{\mu} \to R^{11}_{\mu}(-\omega^{\mu}_{G+}) \ , \tag{28}$$

$$u^2_{\mu} \to R^{11}_{\mu}(\omega^{\mu}_{G+}) \ , \tag{29}$$

$$u_{\mu}v_{\mu} \to R^{12}_{\mu}(\omega^{\mu}_{G+}) \ . \tag{30}$$

Note that Eqs. (16) and (17) do not have the summation $\sum_a$ at this stage. Then the new $G_{\mu}(\omega)$ can be calculated by the matrix inversion of the right-hand side of Eq. (1). Finding the real points satisfying Eq. (18) and calculating Eqs. (20) and (21), one can get new poles $\omega^{\mu a}_{G+}$ and $R^{ij}_{\mu a}(\pm\omega^{\mu a}_{G+})$, $(i, j = 1, 2)$. These are substituted to Eqs. (16) and (17) again, and the procedure is repeated. The converged $G_{\mu}(\omega)$ and $\Sigma_{\mu}(\omega)$ give a solution of Eq. (1). ε_F is determined so as to obtain a right expectation value of the nucleon number $\langle \hat{N} \rangle$ for the nucleus under consideration.

It is worthy to discuss what would happen if the energy denominators in Eqs. (16) and (17) become very small around the poles of the particle Green function. This can happen when the unperturbed energy levels are very dense. Let us ignore pairing correlations for simplicity, and consider the pole $-\omega^{\mu a}_{G+}$. Then we have

$$R^{11}_{\mu a}(-\omega^{\mu a}_{G+}) = \frac{1}{1 - \frac{d}{d\omega} \hbar \Sigma^{11}_{\mu}(\omega) \Big|_{\omega = -\omega^{\mu a}_{G+}}} \ . \tag{31}$$

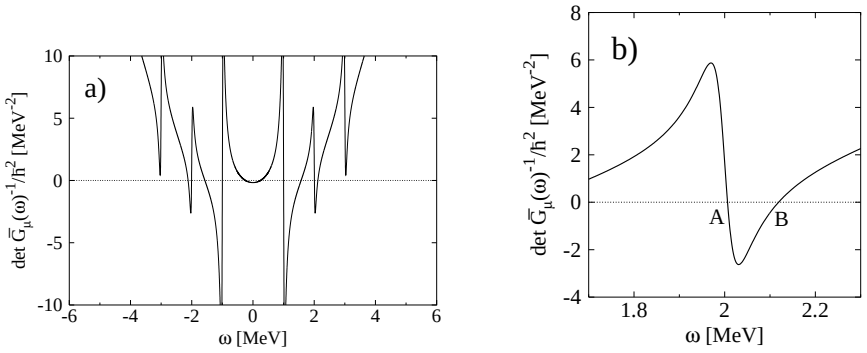

Figure 2. a) Schematic behavior of $\det \overline{G}_\mu^{-1}(\omega)$ on the real axis of ω. b) Magnification in a neighborhood of a singularity.

Thus if the energy denominator of $\Sigma_\mu^{11}(\omega)$ is very small around the pole, then so is $R_{\mu a}^{11}(-\omega_{G+}^{\mu a})$. On the other hand the sum rule of the single-particle strength must be satisfied:

$$\sum_a \left(R_{\mu a}^{11}(-\omega_{G+}^{\mu a}) + R_{\mu a}^{11}(\omega_{G+}^{\mu a}) \right) = 1 \ . \tag{32}$$

Therefore if the small-energy denominators are encountered so often, then the single-particle strength becomes distributed among many poles, leading to a strong fragmentation [50]. This mechanism means a technical advantage of Dyson method because the small-energy denominators do not cause severe problems as can happen in Rayleigh-Schrödinger perturbation theory.

If the ω-dependence of the self-energy $\Sigma_\mu(\omega)$ is ignored, then $\det \overline{G}_\mu^{-1}(\omega)$, see Eq. (19), is a parabola, and there are only two roots in Eq. (18) — that is BCS. With the ω-dependence of $\Sigma_\mu(\omega)$ switched on, $\det \overline{G}_\mu^{-1}(\omega)$ behaves in the way schematically shown in Fig. 2a.

It is seen that the singularities of $\Sigma_\mu(\omega)$ create many poles of $G_\mu(\omega)$. In Fig. 2b we illustrate a magnification in a neighborhood of a singularity. When the averaging parameter η and η_D are finite, the determinant is a continuous function on the real ω axis. It is noted that the zero-point A in Fig. 2b is a spurious pole, because the curve becomes discontinuous at the point A with $\eta, \eta_D \to 0$, and thus the pole disappears. In our experience the residue $R_{\mu a}^{11}(\pm\omega_{G+}^{\mu a})$ for the point A, calculated using Eq. (20), is usually negative.

We note that effect of the off-diagonal Green functions $G_{(nlj)(n' \neq nlj)}$ are assumed small and neglected in this paper. (Cf. [59] and [63])

Now let us consider a field theoretical question related to the anomalous Green function. Is it possible to express diagrams including the anomalous Green functions in terms of the normal Green functions? Let us assume an equation

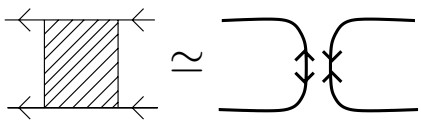

(33)

The left diagram is a two-body Green function carrying the pairing correlations expressed without the anomalous Green functions (see section 34, chapter 7 in [61]).

The ladder diagram of the phonons may be included in the complicated diagram. The right-hand side indicates the anomalous Green functions in the notation of Migdal. (Cf section 1.3.4 in [39].) In this discussion, a line represents not a 2 by 2 matrix but either a normal or a anomalous nucleon Green function. One of components of the correlation energy associated with the solution of Dyson equation can be written, up to a factor, as

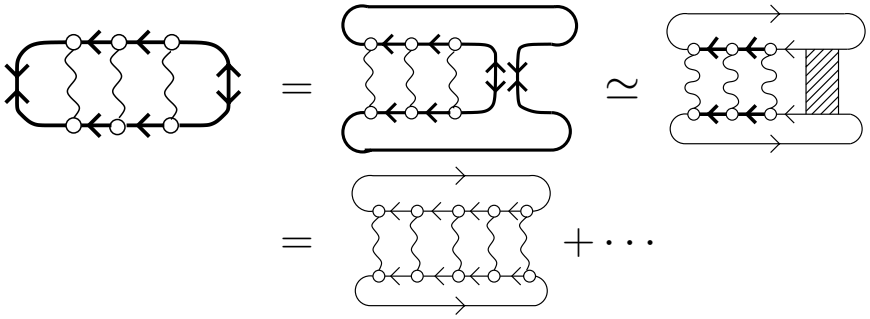

(34)

where the thick lines are perturbed Green functions, and the thin lines are unperturbed ones. Therefore it is seen that the diagrams of the following type are included in the proper self-energy in the Dyson equation:

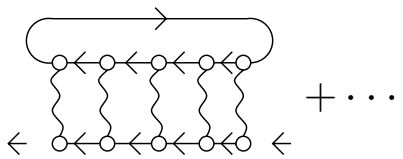

(35)

(See also chap. 2 in [39].)

3 Comparison with a diagonalization of the particle-phonon coupled Hamiltonian

In order to understand this field-theoretical calculation from a viewpoint of a method more familiar to the nuclear-structure physics, we made a comparison with a diagonalization of the Hamiltonian

$$H = H_{\rm par} + H_{\rm coup} + H_{\rm pho} \ , \tag{36}$$

where $H_{\rm par}$ and $H_{\rm pho}$ are unperturbed particle and phonon Hamiltonians, respectively. The particle-phonon coupling $H_{\rm coup}$ was taken from H' in section 6-5a in [3]. We diagonalized H in a space of two particle $\otimes$ 0–2 phonons coupled to the angular momentum $J = 0$. For the particle space we took $\{$ $g_{9/2}$, $d_{5/2}$, $j_{15/2}$ $\}$ above the $N = 126$ shell gap calculated with a Woods-Saxon potential [45]. For phonons we used the lowest 2^+ and 3^- solutions of a QRPA calculation performed using the multipole-multipole force with strengths adjusted so as to reproduce the observed transition probabilities in ^{208}Pb. The coupling strength can also be obtained from the QRPA calculation (cf. sections 6-2c and 6-5a in [3]).

The input energies and vertex are shown in Table I and II, respectively.

Table I. The input energies used in the calculation. ε^0_μ is the unperturbed single-particle energy, and $\hbar\Omega_\lambda$ is the phonon energy.

μ	ε^0_μ [MeV]	λ^π	$\hbar\Omega_\lambda$ [MeV]
$g_{9/2}$	-4.314	2^+	4.10
$j_{15/2}$	-2.490	3^-	2.10
$d_{5/2}$	-1.992		

Table II. The matrix elements of the vertex. The vertex matrix is real and Hermite.

μ	μ'	λ^π	$\left\vert\sqrt{\frac{\hbar}{2\Omega_\lambda B_\lambda}}\langle\mu\vert\vert R_0\frac{dU}{dr}Y_\lambda\vert\vert\mu'\rangle\right\vert$ [MeV]
$g_{9/2}$	$g_{9/2}$	2^+	1.36
$d_{5/2}$	$d_{5/2}$	2^+	0.87
$j_{15/2}$	$j_{15/2}$	2^+	2.24
$g_{9/2}$	$d_{5/2}$	2^+	1.26
$j_{15/2}$	$g_{9/2}$	3^-	4.02

We compare two kinds of quantities. One is the occupation probability of the orbits

$$\begin{aligned} v^2_\mu(\text{Dyson}) &= \sum_{m_\mu}\langle c^\dagger_{\mu m_\mu} c_{\mu m_\mu}\rangle/(2j_\mu+1) \\ &= \sum_a R^{11}_{\mu a}(-\omega^{\mu a}_{G+}) \ , \qquad (37) \\ v^2_\mu(\text{Diag}) &= \sum_X (a_{\mu^2\,X})^2\frac{2}{2j_\mu+1} + \sum_Y (a_{\mu\,Y})^2\frac{1}{2j_\mu+1} \ , \qquad (38) \end{aligned}$$

where $a_{\mu^2\,X}$ and $a_{\mu\,Y}$ are the amplitudes of the components of the ground state $|\,\mathrm{g\,s}\,\rangle$ in the diagonalization method:

$$|\,\mathrm{g\,s}\,\rangle = \sum_X a_{\mu^2\,X}|X\rangle + \sum_Y a_{\mu\,Y}|Y\rangle \ , \qquad (39)$$

$$|X\rangle = [\,|\mu^2\rangle \otimes |0\,, 1\,\text{or}\,2\,\text{phonon}\rangle]_{J\pi=0+} \ , \qquad (40)$$

$$|Y\rangle = [\,|\mu\rangle \otimes |\mu'\neq\mu\rangle \otimes |0\,, 1\,\text{or}\,2\,\text{phonon}\rangle]_{J\pi=0+} \ . \qquad (41)$$

Another quantity to compare is the correlation energy

$$E_{\text{cor}} = E_0 - E^0_{\text{unp}} \ , \qquad (42)$$

Table III. The occupation probabilities of the single-particle orbits v_μ^2 and the correlation energies $E_{\rm cor}$ of the two methods. $\eta = \eta_{\rm D} = 1$ keV and $\varepsilon_F = -4.7908$ MeV were used in the Dyson calculation.

	v_μ^2			$E_{\rm cor}$
	$g_{9/2}$	$j_{15/2}$	$d_{5/2}$	[MeV]
Dyson	0.178	0.013	0.001	−1.62
Diagonalization	0.179	0.013	0.001	−1.53

Table IV. Another set of the input energies.

μ	ε_μ^0 [MeV]	λ^π	$\hbar\Omega_\lambda$ [MeV]
$g_{9/2}$	−3.00	2^+	0.50
$j_{15/2}$	−2.50	3^-	0.50
$d_{5/2}$	−2.00		

where $E_{\rm unp}^0$ is the unperturbed ground-state energy, which is equal to $2\varepsilon_{g9/2}^0$ in the present model. The total energy E_0 is given in the Dyson method by

$$E_0 = \sum_{\mu a} R_{\mu a}^{11}(-\omega_{G+}^{\mu a})(2j_\mu+1)(-\omega_{G+}^{\mu a}) + \varepsilon_F\langle\hat{N}\rangle \ . \tag{43}$$

This equation is derived in Appendix E. The counterpart in the diagonalization method is

$$E_0 = \text{the lowest eigenvalue of } H - \langle H_{\rm pho}\rangle \ . \tag{44}$$

The result is shown in Table III.

It is seen that the two calculations give a nearly-identical result. In order to see difference between the two methods, we used another set of the unperturbed energies artificially changed (see Table IV) keeping the matrix elements of the particle-phonon coupling unchanged.

This choice was made in accordance with the discussion on the fragmentation in section 2. The physical difference between the two models is clear in the distribution of the single-particle strength in Fig. 3.

Given that there are only three particle levels, the latter model (Table IV) is an extremely fragmentation-enhanced model. The correlation energies of the second model is plotted in Fig. 4 (p.13).

We emphasize that Dyson equation is solved nonperturbatively including many poles, so that the many-phonon diagrams are included in the solution. Figure 4 clearly shows this many-phonon effect. It is also noted that the present solution of Dyson equation does not have the vertex correction, while the diagonalization

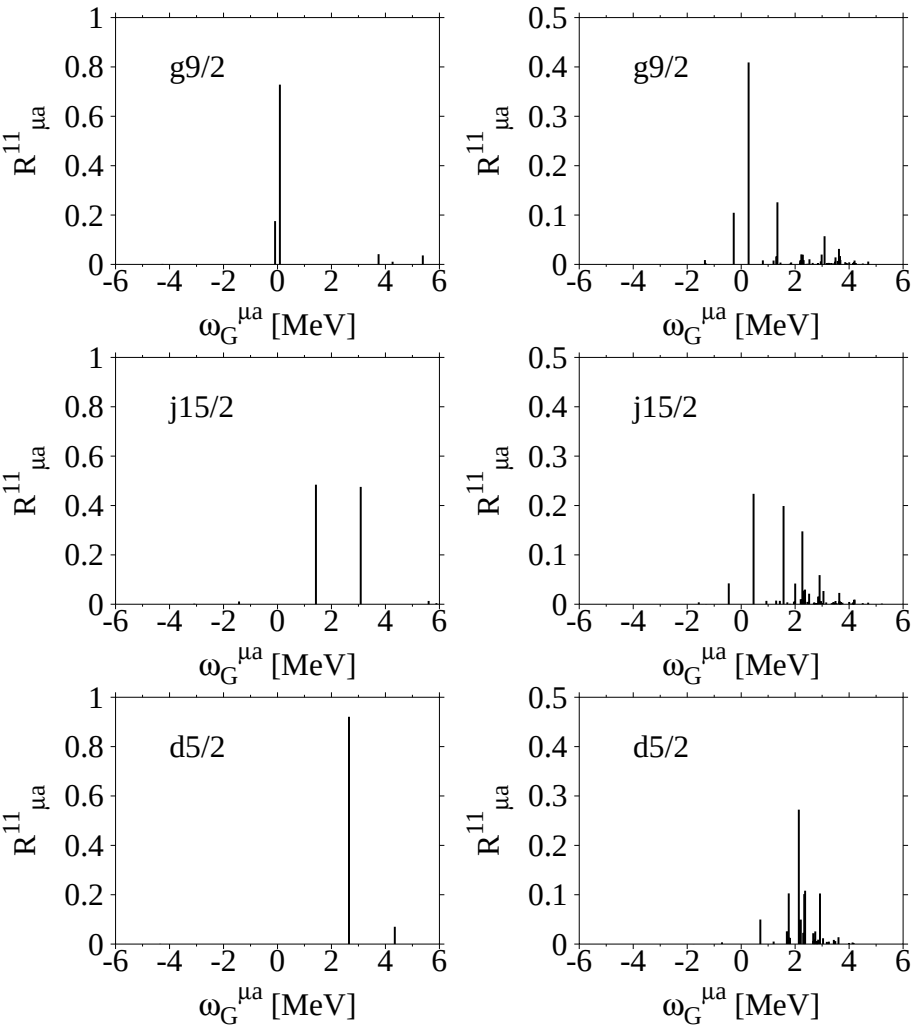

Figure 3. The single-particle strength distribution of the three orbits. $\omega_G^{\mu a}$ means $\pm\omega_{G+}^{\mu a}$. The left three panels are results of the first model (Table I), and the right three are of the second model (Table IV). Note the difference in the vertical scale.

method includes the effect within the order of 2-phonon. Thus the truncation scheme in the actual calculation is in fact different between the two methods. Given this difference, the comparisons show that the two methods are consistent.

In our solution, the number of the poles of the particle Green functions can vary from one step to another in the iteration process, and due to this reason small fluctuations are unavoidable. In most calculations presented in this paper, including those of the next section, the errors in the pairing gaps and perturbed single-particle energies of the quasiparticle poles in the valence shell are negligible.

4 Pairing gaps in ^{120}Sn

In the wake of the above calculation, we have performed a more realistic study, calculating the neutron pairing gap of ^{120}Sn using the Dyson equation. (A part of

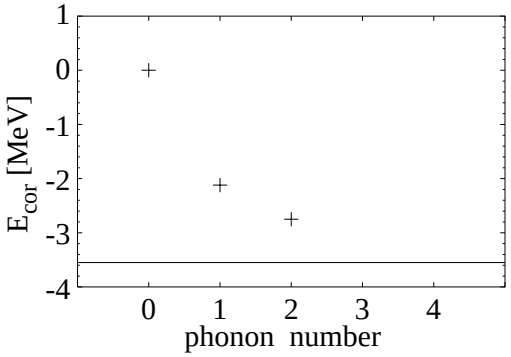

Figure 4. The correlation energies of the Dyson equation ($E_{\rm cor} = -3.55 \pm 0.01$ MeV, the mean value is shown by the line. For the error, see text.) and the diagonalization method (the crosses) obtained for the input in Table IV. The horizontal axis is the maximum phonon number in the basis states used in the diagonalization, e. g., phonon number = 1 means that the basis state is $[\,|\mu\mu'\rangle \otimes |0\,\text{or}\,1\text{phonon}\rangle\,]_{J\pi=0+}$. $E_{\rm cor}$ of the Dyson method corresponds to a large phonon number (see the text). $\varepsilon_F = -4.280$ MeV was used. η and $\eta_{\rm D}$ are unchanged.

this calculation has been published in a compact way in [64].) In this calculation the single-particle basis covers all of the bound energy region starting from the orbital $1s_{1/2}$. We used the unperturbed single-particle spectra

$$\varepsilon^0_\mu = \frac{m}{m_{\rm k}}(\varepsilon^{\rm WS}_\mu - \varepsilon_F) + \varepsilon_F \ , \tag{45}$$

with $m_{\rm k} = 0.7m$ and $\varepsilon^{\rm WS}_\mu$ being Woods-Saxon spectra, for avoiding double counting of the particle-phonon coupling effect. (Cf. section 4.6.3 in [35].)

The computation time needed for our calculations depends strongly on the number of phonon modes λn included. The full QRPA response for the multipolarities $\lambda^\pi = 2^+, 3^-, 4^+, 5^-$ in the energy interval 0–20 MeV used in ref. [45] consists of about two hundreds phonon modes of energies $\hbar\Omega_{\lambda n}$ and zero-point amplitudes $\beta_{\lambda n}$ for each multipolarity. We include the four lowest phonons, one for each multipolarity, which give the largest contributions to the induced phonon interaction. We account for the effects of the other roots including only a few effective phonons of energy $\hbar\Omega^{\rm eff}_{\lambda n}$, distributed in the interval 0–20 MeV, choosing their effective strength so that when they are used in the Bloch-Horowitz calculation of ref. [45] they reproduce the state-dependent gap obtained there. This is obtained, considering that the sum of the (asymmetrized) matrix elements of the induced interaction between two pairs $(j_\nu)^2_{J=0}, (j_{\nu'})^2_{J=0}$ due to the phonons lying in an energy interval $[\Omega_a, \Omega_b]$, calculated according to the Bloch-Horowitz formalism, is given by

$$v_{\nu\nu'} = \frac{|\langle\nu'||R_0\frac{\partial U}{\partial r}||\nu\rangle|^2}{(2j_\nu+1)(2j_{\nu'}+1)(2\lambda+1)} \sum_{\Omega_{\lambda n}=\Omega_a}^{\Omega_b} \frac{4\beta^2_{\lambda n}}{E_{\rm cor} - (e_\nu + e_{\nu'} + \hbar\Omega_{\lambda n})} \ , \tag{46}$$

where $E_{\rm cor}$ and e_ν are the correlation energy of the ground state and the absolute value of the single-particle energy with respect to the Fermi level, respectively. The

Table V. The energies of the phonon modes $\hbar\Omega^{\rm eff}_{\lambda n}$ and coupling strength $\beta^{\rm eff}_{\lambda n}/\sqrt{2\lambda+1}$. Tables a), b), c) and d) are for $\lambda^\pi = 2^+$, 3^-, 4^+ and 5^-, respectively. The lowest-energy modes ($n = 1$) were taken from a QRPA calculation directly. The coupling strengths as well as the energies of the other modes were determined by the procedure shown in Eqs. (46) and (47).

a)

$\lambda^\pi = 2^+$		
n	$\hbar\Omega^{\rm eff}_{\lambda n}$ [MeV]	$\beta^{\rm eff}_{\lambda}/\sqrt{2\lambda+1}$
1	1.173	0.0554
2	5.2	0.0134
3	12.5	0.0447

b)

$\lambda^\pi = 3^-$		
n	$\hbar\Omega^{\rm eff}_{\lambda n}$ [MeV]	$\beta^{\rm eff}_{\lambda}/\sqrt{2\lambda+1}$
1	2.423	0.0591
2	5.57	0.0317
3	10.0	0.0238
4	21.0	0.0291

c)

$\lambda^\pi = 4^+$		
n	$\hbar\Omega^{\rm eff}_{\lambda n}$ [MeV]	$\beta^{\rm eff}_{\lambda}/\sqrt{2\lambda+1}$
1	2.470	0.0248
2	8.0	0.0300
3	12.0	0.0300
4	15.0	0.0270

d)

$\lambda^\pi = 5^-$		
n	$\hbar\Omega^{\rm eff}_{\lambda n}$ [MeV]	$\beta^{\rm eff}_{\lambda}/\sqrt{2\lambda+1}$
1	2.402	0.0250
2	8.0	0.0365
3	13.0	0.0166
4	21.0	0.0232

effective strength of the phonon representing this interval is then chosen so as to satisfy the equations

$$\frac{(\beta^{\rm eff}_{\lambda n})^2}{E_{\rm cor} - (e_\nu + e_{\nu'} + \hbar\Omega^{\rm eff}_{\lambda n})} = \sum_{\Omega_{\lambda n}=\Omega_a}^{\Omega_b} \frac{\beta^2_{\lambda n}}{E_{\rm cor} - (e_\nu + e_{\nu'} + \hbar\Omega_{\lambda n})} \ , \tag{47a}$$

$$\hbar\Omega^{\rm eff}_{\lambda n} = \hbar\Omega_b \ , \tag{47b}$$

for the pairs $(j_\nu)^2_{J=0}, (j_{\nu'})^2_{J=0}$ giving the largest contribution to the pairing gap for the multipolarity λ. The energies and zero-point amplitudes of the effective phonons are listed in Table V, divided by $\sqrt{2\lambda+1}$.

Then the coupling strength

$$\sqrt{\frac{\hbar}{2\Omega^{\rm eff}_{\lambda n} B^{\rm eff}_{\lambda n}}} = \frac{\beta^{\rm eff}_{\lambda n}}{\sqrt{2\lambda+1}} \ ,$$

is used for Eq. (10). The BCS+Bloch-Horowitz calculation performed with this restricted ensemble of phonons reproduces the state-dependent pairing gaps of ref. [45] within a few per cent.

Below, results obtained with the fixed imaginary parameter $\eta = \eta_0 = -\mathrm{Im}\,\omega^{\mu a}_{G+} =$ 1 keV are shown. In the present calculation the maximum number of poles with respect to μ is $\sim$200. The sum rule of the single-particle strength, Eq. (32), is satisfied by more than 90 % in average in the orbits in the valence shell. The computations have been performed on a parallel computer. In fact the Green function method is well suited for parallel computation, because the pole search of each orbit can be done separately.

A few self-checks are possible on the accuracy of the solution of Dyson equation. The self-energy is a functional of the particle Green function, and if this Green function, represented by Eqs. (12)–(15), is identical to $(\, G^{0\,-1}_{\mu}(\omega) - \Sigma_{\mu}(\omega)\,)^{-1}$, then the Green function is a solution. Such a direct check is shown in Fig. 5 for the orbits in the valence shell around the Fermi level.

It is seen that the accuracy is good. Another check is Eq. (136) in Appendix C. This equation is satisfied with good accuracy.

We show the calculated pairing gaps in Fig. 6 (p.17).

The value of the gap of $2\mathrm{d}_{5/2}$ is mostly determined by the off-diagonal element of Eq. (10) with $\mu' = 1\mathrm{h}_{11/2}$ and $\lambda^{\pi} = 3^{-}$. Therefore $|R^{12}_{1\mathrm{h}11/2}(\omega^{1\mathrm{h}11/2\,a_0}_{G+})| = 0.35$ of the quasiparticle pole[3] [3] a_0 plays an important role not only for $\Delta_{1\mathrm{h}11/2}$ but also for $\Delta_{2\mathrm{d}5/2}$. On the other hand $|R^{12}_{2\mathrm{d}5/2}(\omega^{2\mathrm{d}5/2\,a_0}_{G+})|$ is 0.04, thus the influence of $2\mathrm{d}_{5/2}$ on $\Delta_{1\mathrm{h}11/2}$ is small.

The average of the pairing gaps in the valence shell is 0.54 MeV in the present calculation. This may be compared with the value of 1.39 MeV deduced from the observed odd-even mass difference as well as the average gap of 0.82 MeV obtained in ref. [45].

The poles $\pm\omega^{\mu a}_{G+}$ of the Green function G^{11} are distributed symmetrically with respect to the Fermi surface ($\omega = 0$). The spectral function of the orbits in the valence shell are illustrated in Fig. 7 (p.18). The single-particle picture is rather good for most orbits, except for the $d_{5/2}$ whose sinlge-particle strength is split into several peaks. Most orbits have a pronounced hole- or particle-character, except for for the $h_{11/2}$ which displays two large peaks on either side of the Fermi energy. It is to be noted that for this orbit the single-particle strength for the two quasiparticle poles is only 0.73. The third not negligible peak close to ω =2 MeV may be associated with the quasiparticle plus a collective state.

It is seen from Eq. (112) in Appendix C that the peaks in $\omega < 0$ part of the spectral function are associated with a pick-up reaction and those in the $\omega > 0$ part with a stripping reaction. Thus the spectral functions of Fig. 7, can be rearranged as shown into Fig. 8 (p.19) for the case of $h_{11/2}$.

If each excited state can be resolved, the definition of E_x is $E_0 - E_i$, where E_0 is the ground-state total energy of the neutrons in ^{120}Sn relative to $\varepsilon_F\langle\hat{N}\rangle$, and E_i is defined in the same way as E_0 but for various states of ^{119}Sn and ^{121}Sn. If strong signals are observed in both pick-up and stripping reactions for the same orbit near the Fermi level with the same E_x, this would be a clear indication of pairing correlations.

The particle-phonon coupling influences of course also the single-particle spec-

[3] A pole, or a pair of poles if the pairing gap is not zero, which carries the largest, or major, single-particle strength $R^{11}_{\mu a}(\omega^{\mu a}_{G+}) + R^{11}_{\mu a}(-\omega^{\mu a}_{G+})$.

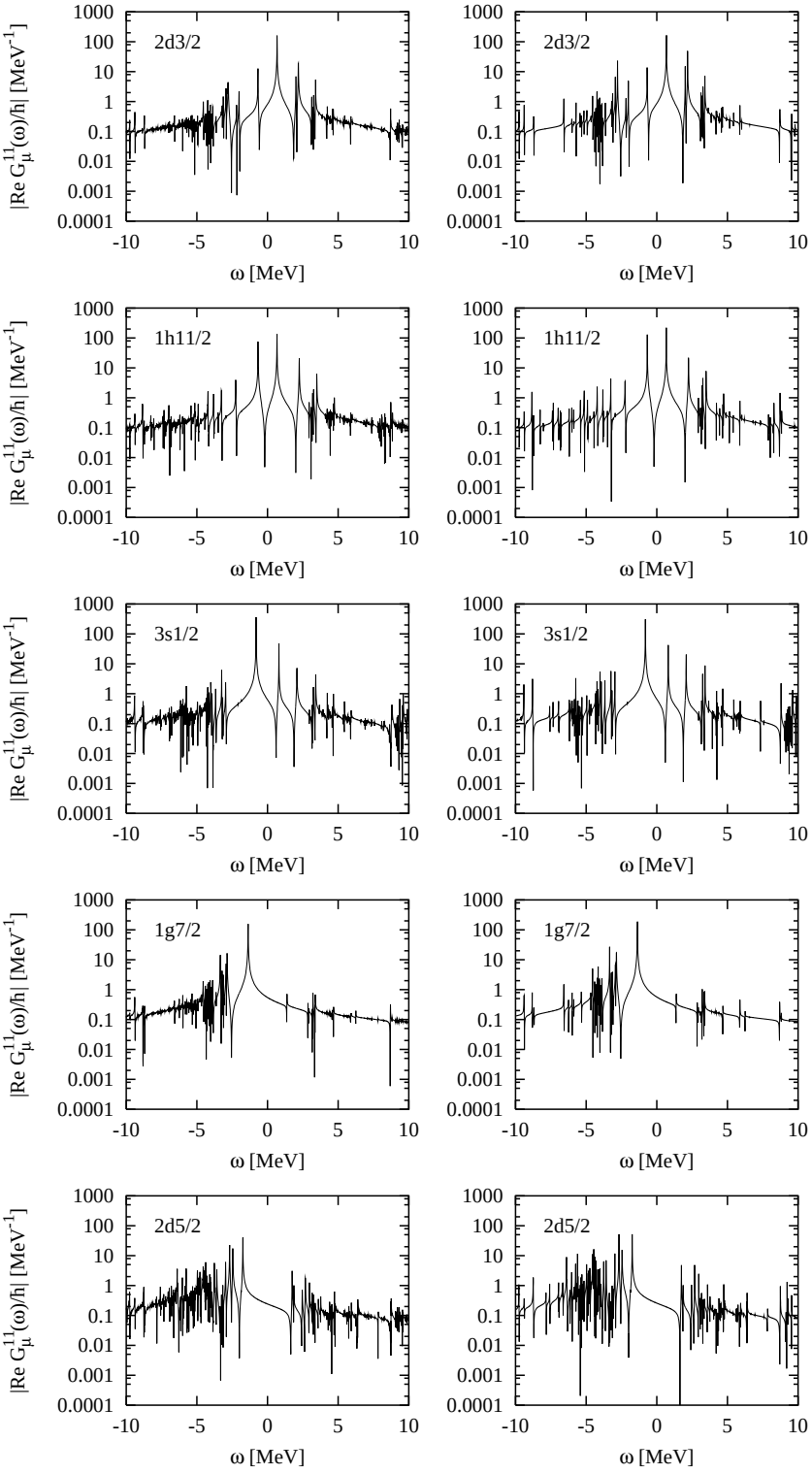

Figure 5. Absolute value of the real part of $G_\mu^{11}(\omega)/\hbar$ in log scale. The left column shows $\left|\left[(\,\hbar G_\mu^{0\,-1}(\omega) - \hbar\Sigma_\mu(\omega)\,)^{-1}\right]_{11}\right|$, and the right column illustrates those given by Eq. (12).

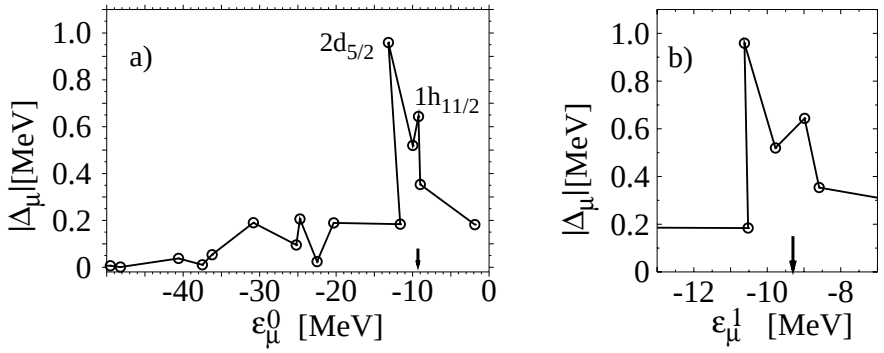

Figure 6. a) Absolute values of the pairing gaps of the neutron of ^{120}Sn in the calculation of the Dyson method shown as a function of ε^0_μ. The gap is obtained according to Eq. (158) in Appendix F. The arrow indicates the location of the Fermi level. b) $|\Delta_\mu|$ as a function of the perturbed single-particle energy ε^1_μ (see Eq. (160) in Appendix F) in the vicinity of the Fermi level.

trum. We show the perturbed as well as unperturbed spectra in Fig. 9 (p.19).

The increase in the level density in the vicinity of the Fermi level is a known effect of the coupling (section 4 in [35]).

We calculated also the pairing energy (see Appendix E):

$$E_{\rm pair} = -i\sum_\mu (2j_\mu+1)\frac{1}{2}\int_{-\infty}^{\infty}\frac{d\omega}{2\pi}\left(\hbar\Sigma^{12}_\mu(\omega)\frac{1}{\hbar}G^{21}_\mu(\omega)e^{i\eta\omega}+\hbar\Sigma^{21}_\mu(\omega)\frac{1}{\hbar}G^{12}_\mu(\omega)e^{-i\eta\omega}\right)\ , \tag{48}$$

and obtained $E_{\rm pair} = -3.9$ MeV.

5 BCS approximation

This approximation was introduced in section 2 as the initial guess for solving Dyson equation. From the viewpoint of Green function method, BCS approximation is a normalized-quasiparticle approximation. Thus, generally speaking, if the single-particle strength is well concentrated on the quasiparticle pole, then BCS may be a good approximation. As was discussed in section 2, if the self-energy has no ω-dependence, then the single-particle strength is distributed to only two poles at most.

Next we compare analytically the present Dyson calculation and the BCS + Bloch-Horowitz calculation in [45]. One of the differences is, as was mentioned, that $R^{12}_{\mu a_0}(\omega^{\mu a_0}_{G+})$ (a_0 denotes the quasiparticle pole) differs from $u_\mu v_\mu$ in BCS due to the fragmentation of the single-particle strength. The second difference is the deviation of the function $Z_\mu(\omega^{\mu a_0}_{G+})$, Eq. (154) in Appendix F, from 1. A third difference is the energy denominator in the gap equation. If one puts for simplicity $\hbar\Sigma^{12}_\mu(\omega^{\mu a_0}_{G+}) \simeq \Delta_\mu$, $R^{12}_{\mu a_0}(\omega^{\mu a_0}_{G+}) \simeq u_\mu v_\mu$ and $\omega^{\mu a_0}_{G+} \simeq \mathcal{E}_\mu$, the pairing gap in Dyson method can be written

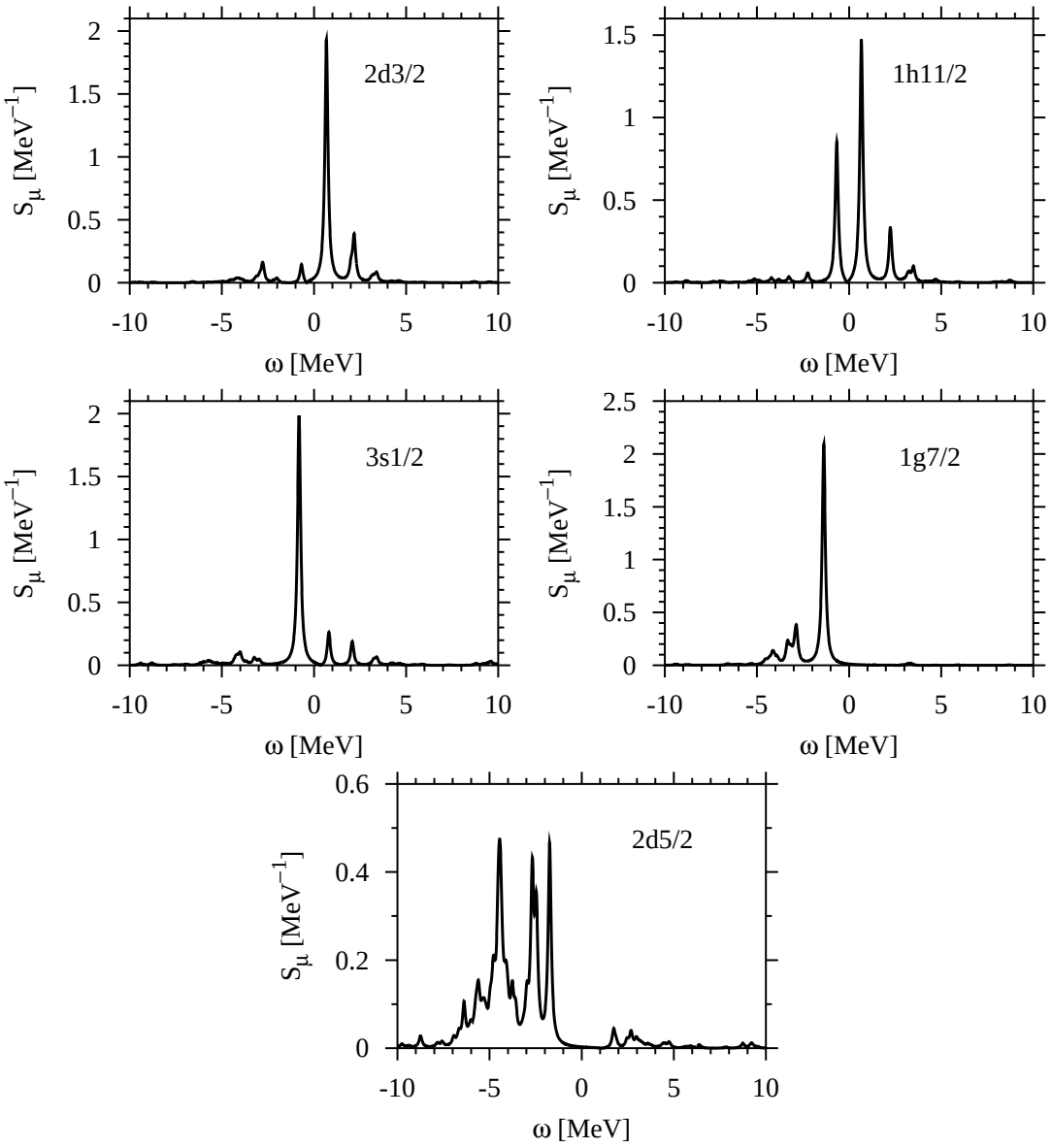

Figure 7. The spectral function $S_\mu(\omega) = \left|\mathrm{Im}\, G^{11}_\mu(\omega)/\hbar\right|/\pi$ for the orbits in the valence shell. The poles and residues of the solution were inserted into Eq. (12) with $\mathrm{Im}\,\omega^{\mu a}_{G+} = -100$ keV. $\omega = 0$ corresponds to the Fermi level.

as

$$\Delta_\mu \simeq -\sum_{\lambda n}\sum_{\mu'} \frac{\hbar}{2\Omega_{\lambda n}B_{\lambda n}}\frac{1}{2j_\mu+1}\left|\langle\mu||R_0\frac{dU}{dr}Y_\lambda||\mu'\rangle\right|^2 u_{\mu'}v_{\mu'} \times\left\{\frac{1}{-\mathcal{E}_\mu-\mathcal{E}_{\mu'}-\hbar\Omega_{\lambda n}}+\frac{1}{\mathcal{E}_\mu-\mathcal{E}_{\mu'}-\hbar\Omega_{\lambda n}}\right\}. \quad (49)$$

On the other hand, the gap of BCS + Bloch-Horowitz calculation leads to

$$\Delta_\mu(\mathrm{BCS+BH}) = -\sum_{\lambda n}\sum_{\mu'} \frac{\hbar}{2\Omega_{\lambda n}B_{\lambda n}}\frac{1}{2j_\mu+1}\left|\langle\mu||R_0\frac{dU}{dr}Y_\lambda||\mu'\rangle\right|^2 u_{\mu'}v_{\mu'}$$

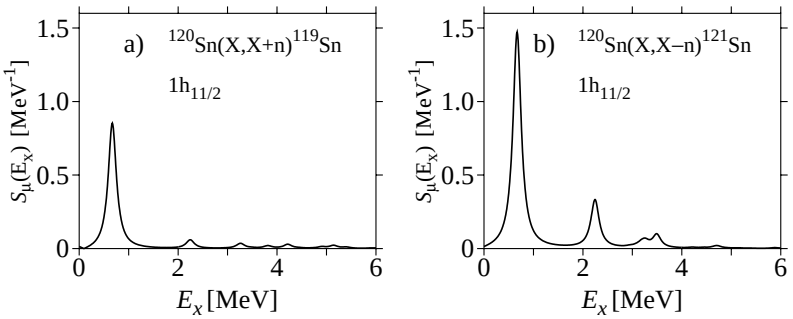

Figure 8. The spectral functions of the neutron $1h_{11/2}$ as functions of $E_x = |\omega|$. a) hole type b) particle type.

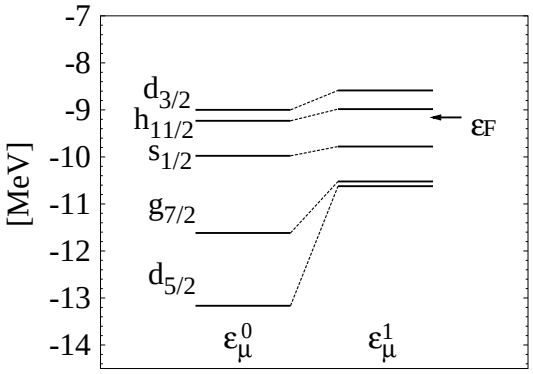

Figure 9. The unperturbed (ε^0_μ) and perturbed (ε^1_μ) single-particle spectra associated with the quasiparticle poles. ε^1_μ is defined in Eq. (160) in Appendix F.

$$\times \frac{2}{E_{\rm cor} - (|\tilde{\varepsilon}^0_\mu| + |\tilde{\varepsilon}^0_{\mu'}| + \hbar\Omega_{\lambda n})} \ , \tag{50}$$

where $E_{\rm cor}$ is the correlation energy of the perturbed ground state. Thus, the essential difference, in the no correlation limit, is the sign of $\mathcal{E}_\mu$ in the second energy denominator in Eq. (49).

Eq. (48) may be compared to the pairing energy in the BCS approximation:

$$E_{\rm pair}({\rm BCS}) = \sum_{\mu\mu'} \frac{(2j_\mu+1)(2j_{\mu'}+1)}{4} u_\mu v_\mu u_{\mu'} v_{\mu'} V_{\mu\mu'} \ , \tag{51}$$

$$V_{\mu\mu'} = \langle (\mu' m_{\mu'})\overline{(\mu' m_{\mu'})}|V|(\mu m_\mu)\overline{(\mu m_\mu)}\rangle_{\rm antisymmetrized} \ . \tag{52}$$

We obtained $E_{\rm pair}({\rm BCS}) = -4.6$ MeV in the BCS + Bloch-Horowitz calculation.

6 Summary

In this paper we have investigated the effect of particle-phonon coupling on nuclear pairing correlations in detail. The dynamical equation treated is Dyson equation

including the anomalous Green function. We showed the formulation from the viewpoint to clarify how to solve the equation in such a way that the effect beyond BCS is not suppressed. The comparison was made between the solutions of Dyson equation and diagonalization of the particle-phonon coupled Hamiltonian, and we clarified both difference and similarity. The difference is in the truncation scheme, and nonperturbative effect can be taken into account for a class of diagrams in Dyson method by solving the equation iteratively. The similarity of the solutions is clear when the model does not have strong the fragmentation effect of the single-particle strength. We have solved Dyson equation for the neutrons in ^{120}Sn and calculated the pairing gaps. The average pairing gap near the Fermi level arising from the phonon-induced interaction is around 40 % of the observed gap from the odd-even mass difference. According to the spectral functions the quasiparticle picture is not perfect but acceptable for many of the single-particle orbits near the Fermi level except for $2d_{5/2}$. This level is more than 2 MeV below the Fermi level, however, the orbit has the appreciable magnitude of the pairing gap. This gap arises mainly from the 3^- phonon coupling, of which the vertex matrix has only off-diagonal elements. For this reason the pairing gap as a function of the unperturbed single-particle energy does not have a completely-smooth shape peaked at the Fermi level. As for the overall shape, the pairing gap arising from the phonon-induced interaction is of the surface type.

We have discussed also the BCS + Bloch-Horowitz calculation. The mechanism to avoid divergence possibly arising from small energy denominator is different between Dyson calculation and BCS + Bloch-Horowitz method. The latter method has always negative, i. e. non-zero, energy denominators in the pairing gap.

Several further steps are needed, in order to obtain a complete quantitative assessment of the contribution of the particle-phonon coupling to the nuclear pairing correlations. First, the vertex correction of the self-energy should be investigated. In fact, our present calculation is partially nonperturbative and partially perturbative. Needless to say, it is a nonperturbative effect that the pairing gaps were obtained using the single-particle basis. On the other hand, the vertex was treated in the lowest perturbation.

It will be necessary also to combine the phonon-induced interaction with a bare NN interaction into the self-energy for understanding the nuclear pairing correlations fully microscopically, and to look for an adequate Hartree-Fock basis consistent with the effective mass arising from the particle-phonon coupling. One may be also concerned with breaking of the particle-number conservation. Since we calculate the pairing gap in a finite-body system, the particle number is not conserved.

Appendix A – diagram rule –

The original Nambu-Gor'kov formulation assumes that the spin up or down is a good quantum number [43] . In this appendix we show in detail a derivation of the diagram rule without this condition. We derive the rule by making an expansion of a perturbed nucleon Green function using products of unperturbed nucleon Green functions [62]. It is noted that the nonperturbative effect of Dyson equation is essential for getting the anomalous Green function if unpaired states are used as the basis.

We put

$$\Psi_\nu = \begin{pmatrix} c_\nu \\ c^\dagger_{\overline{\nu}} \end{pmatrix} \ . \tag{53}$$

In this appendix ν is a single-particle index of a complete basis, and $\overline{\nu}$ is a time-reversed state of ν. Note that $\{\nu_i\}_{i=\cdots} = \{\overline{\nu}_i\}_{i=\cdots}$, and we do not impose any explicit good quantum number on the basis as long as a general diagram rule is discussed. Let us consider the particle-phonon coupling Hamiltonian (see sections 6.2b and 6.3a in [3]):

$$\hat{H}_{\rm int} = \sum_{lm} \kappa_l \hat{\alpha}_{lm} \sum_{\mu\nu} \langle \mu | F^\dagger_{lm} | \nu \rangle \frac{1}{2} \Psi^\dagger_\mu \tau_3 \Psi_\nu \ , \tag{54}$$

where

$$F_{lm} = -R_0 \frac{1}{\kappa_l} \frac{dU(r)}{dr} Y_{lm}(\theta, \varphi) \ , \tag{55}$$

$$\hat{\alpha}_{lm} = (\alpha_l)_0 \, (c^\dagger_{lm} + c_{\overline{lm}}) \ , \tag{56}$$

$$(\alpha_l)_0 = \langle lm | F_{lm} | 0 \rangle = \sqrt{\frac{\hbar}{2 B_l \Omega_l}} \ , \tag{57}$$

$$\kappa_l = \int dr \ r^2 R_0 \frac{d\rho_0(r)}{dr} R_0 \frac{dU(r)}{dr} \ . \tag{58}$$

R_0 is a mean nuclear radius, and $U(r)$ is a nuclear potential. $c^\dagger_{lm}$ is a creation operator of a phonon specified by the multipolarity l and its z-component m. We define $c_{\overline{lm}} = (-)^m c_{l\,-m}$. $(\alpha_l)_0$ is a zero-point amplitude of the phonon, which is related to the inertia parameter B_l and the phonon energy $\hbar\Omega_l$. $|lm\rangle$ and $|0\rangle$ are a one-phonon and zero-phonon state, respectively. $\rho_0(r)$ denotes a nuclear density in the equilibrium.

With a relation

$$\langle \mu | F^\dagger_{lm} | \nu \rangle \ = \ \langle \overline{\nu} | F^\dagger_{lm} | \overline{\mu} \rangle \ , \tag{59}$$

it follows that

$$\sum_{\mu\nu} \langle \mu | F^\dagger_{lm} | \nu \rangle \frac{1}{2} \Psi^\dagger_\mu \tau_3 \Psi_\nu \ = \ \sum_{\mu\nu} \langle \mu | F^\dagger_{lm} | \nu \rangle \frac{1}{2} (c^\dagger_\mu c_\nu - c_{\overline{\mu}} c^\dagger_{\overline{\nu}}) \tag{60}$$

$$= \ \sum_{\mu\nu} \langle \mu | F^\dagger_{lm} | \nu \rangle c^\dagger_\mu c_\nu + \text{const} \ . \tag{61}$$

That is, since the particle-phonon coupling considered here does not depend on the spin, Nambu-Gor'kov formalism can be introduced without much extension.

We introduce a time-dependent coupling in the interaction picture:

$$\hat{H}_{\rm int}(t) = \sum_{lm} \kappa_l \hat{\alpha}_{lm}(t) \sum_{\mu\nu} \langle \mu | F^\dagger_{lm} | \nu \rangle \frac{1}{2} \Psi^\dagger_\mu(t) \tau_3 \Psi_\nu(t) \ , \tag{62}$$

where the time-dependent operators are defined as

$$\hat{\alpha}_{lm}(t) = e^{i\hat{H}^{\rm ph}_0 t/\hbar} \hat{\alpha}_{lm} e^{-i\hat{H}^{\rm ph}_0 t/\hbar} \ , \tag{63}$$

$$\Psi^\dagger_\mu(t) = e^{i\hat{H}_0 t/\hbar} \Psi^\dagger_\mu e^{-i\hat{H}_0 t/\hbar} \ . \tag{64}$$

$\hat{H}_0^{\rm ph}$ and $\hat{H}_0$ are unperturbed Hamiltonians of the phonon and single-particle relative to the Fermi level, respectively. The basic formula from which we start is

$$\begin{aligned} iG(t) &= \begin{pmatrix} iG^{11}_{\nu\mu}(t) & iG^{12}_{\nu\overline{\mu}}(t) \\ iG^{21}_{\overline{\nu}\mu}(t) & iG^{22}_{\overline{\nu}\overline{\mu}}(t) \end{pmatrix} \\ &= \sum_{m=0}^{\infty} \left(\frac{-i}{\hbar}\right)^m \frac{1}{m!} \int_{-\infty}^{\infty} dt_1 \cdots \int_{-\infty}^{\infty} dt_m \\ &\quad \times \langle \Phi_0 | \mathrm{T}\left[\hat{H}_{\rm int}(t_1)\hat{H}_{\rm int}(t_2)\cdots\hat{H}_{\rm int}(t_m)\Psi_\nu(t)\Psi^\dagger_\mu\right]|\Phi_0\rangle_{\rm connected} \ . \end{aligned} \tag{65}$$

$\mathrm{T}[\cdots]$ is the time-ordered product, and the meaning of "connected" shall be clearest in the diagram later. $|\Phi_0\rangle$ denotes an unperturbed ground state of the system of the single-particles and phonons. It is assumed $c_\mu|\Phi_0\rangle = c_{lm}|\Phi_0\rangle = 0$. The $m = 0$ term is $\langle\Phi_0|\mathrm{T}[\Psi_\nu(t)\Psi^\dagger_\mu]|\Phi_0\rangle = iG_0(t)$. Since the unperturbed Hamiltonian does not have the coupling, we have

$$|\Phi_0\rangle = |\Phi_0^{\rm n}\rangle|\Phi_0^{\rm ph}\rangle \ , \tag{66}$$

where $|\Phi_0^{\rm n}\rangle$ and $|\Phi_0^{\rm ph}\rangle$ are the ground states of the single-particles and phonons, respectively. The derivation of the formula (65) is not affected by the inclusion of the anomalous Green function. (See, e. g., [62] for the derivation.)

By inserting Eq. (62) to Eq. (65) and using Wick theorem, it follows that

$$\begin{aligned} &\begin{pmatrix} iG^{11}_{\nu\mu}(t) & iG^{12}_{\nu\overline{\mu}}(t) \\ iG^{21}_{\overline{\nu}\mu}(t) & iG^{22}_{\overline{\nu}\overline{\mu}}(t) \end{pmatrix} \\ = &\sum_{m=0}^{\infty} \left(\frac{-i}{\hbar}\right)^m \frac{1}{m!} \int_{-\infty}^{\infty} dt_1 \cdots \int_{-\infty}^{\infty} dt_m \frac{1}{2^m} \\ &\times \sum_{l_1 m_1} \kappa_{l_1} \sum_{\nu_1\mu_1} \langle\mu_1|F^\dagger_{l_1 m_1}|\nu_1\rangle \cdots \sum_{l_m m_m} \kappa_{l_m} \sum_{\nu_m\mu_m} \langle\mu_m|F^\dagger_{l_m m_m}|\nu_m\rangle \\ &\times \langle\Phi_0^{\rm ph}|\mathrm{T}\left[\hat{\alpha}_{l_1 m_1}(t_1)\hat{\alpha}_{l_2 m_2}(t_2)\cdots\hat{\alpha}_{l_m m_m}(t_m)\right]|\Phi_0^{\rm ph}\rangle \\ &\times \langle\Phi_0^{\rm n}|\mathrm{T}\left[\Psi^\dagger_{\mu_1}(t_1)\tau_3\Psi_{\nu_1}(t_1)\Psi^\dagger_{\mu_2}(t_2)\tau_3\Psi_{\nu_2}(t_2)\cdots\Psi^\dagger_{\mu_m}(t_m)\tau_3\Psi_{\nu_m}(t_m)\Psi_\nu(t)\Psi^\dagger_\mu\right]|\Phi_0^{\rm n}\rangle_{\rm conn.} \\ = &\sum_{m=0}^{\infty} \left(\frac{-i}{\hbar}\right)^m \frac{1}{m!} \int_{-\infty}^{\infty} dt_1 \cdots \int_{-\infty}^{\infty} dt_m \frac{1}{2^m} \\ &\times \sum_{l_1 m_1} \kappa_{l_1} \sum_{\nu_1\mu_1} \langle\mu_1|F^\dagger_{l_1 m_1}|\nu_1\rangle \cdots \sum_{l_m m_m} \kappa_{l_m} \sum_{\nu_m\mu_m} \langle\mu_m|F^\dagger_{l_m m_m}|\nu_m\rangle \\ &\times \langle\Phi_0^{\rm ph}|\hat{\alpha}_{l_1 m_1}(t_1)\hat{\alpha}_{l_2 m_2}(t_2) \quad \cdots \quad \hat{\alpha}_{l_m m_m}(t_m) \\ &\qquad \text{+ all other possible full contractions}|\Phi_0^{\rm ph}\rangle \\ &\times \langle\Phi_0^{\rm n}|\Psi^\dagger_{\mu_1}(t_1)\,\tau_3\Psi_{\nu_1}(t_1) \quad \cdots \quad \Psi^\dagger_{\mu_m}(t_m)\,\tau_3\Psi_{\nu_m}(t_m)\Psi_\nu(t)\Psi^\dagger_\mu \\ &\qquad \text{+ all other possible full contractions}|\Phi_0^{\rm n}\rangle_{\rm conn} \ . \end{aligned} \tag{67}$$

Let us show an example how the contraction of the type $\Psi_\nu\,(\cdots)\,\Psi_{\nu'}$ can be treated:

$$\langle\Phi_0^{\rm n}|\Psi^\dagger_{\mu_1}(t_1)\tau_3\Psi_{\nu_1}(t_1)(\cdots)\Psi^\dagger_{\mu_i}(t_i)\tau_3\Psi_{\nu_i}(t_i)\cdots|\Phi_0^{\rm n}\rangle$$

$$
\begin{aligned}
&= \langle\Phi_0^{\rm n}|\Psi^\dagger_{\mu_1}(t_1)\tau_3 \begin{pmatrix} c_{\nu_1}(t_1)(\cdots)c^\dagger_{\mu_i}c_{\nu_i}(t_i) - c_{\nu_1}(t_1)(\cdots)c_{\overline{\mu}_i}(t_i)c^\dagger_{\overline{\nu}_i}(t_i) \\ c^\dagger_{\overline{\nu}_1}(t_1)(\cdots)c^\dagger_{\mu_i}(t_i)c_{\nu_i}(t_i) - c^\dagger_{\overline{\nu}_1}(t_1)(\cdots)c_{\overline{\mu}_i}(t_i)c^\dagger_{\overline{\nu}_i}(t_i) \end{pmatrix} \cdots |\Phi_0^{\rm n}\rangle \\
&= \langle\Phi_0^{\rm n}|\Psi^\dagger_{\mu_1}(t_1)\,\tau_3 \begin{pmatrix} c_{\nu_1}(t_1)(\cdots)c^\dagger_{\overline{\nu}_i}(t_i) & c_{\nu_1}(t_1)(\cdots)c_{\nu_i}(t_i) \\ c^\dagger_{\overline{\nu}_1}(t_1)(\cdots)c^\dagger_{\overline{\nu}_i}(t_i) & c^\dagger_{\overline{\nu}_1}(t_1)(\cdots)c_{\nu_i}(t_i) \end{pmatrix} \begin{pmatrix} c_{\overline{\mu}_i}(t_i) \\ -c^\dagger_{\mu_i}(t_i) \end{pmatrix} \\
&\quad \cdots|\Phi_0^{\rm n}\rangle \\
&= \langle\Phi_0^{\rm n}|\Psi^\dagger_{\mu_1}(t_1)\,\tau_3\Psi_{\nu_1}(t_1)(\cdots)\Psi^\dagger_{\overline{\nu}_i}(t_i)\tau_3\Psi^\dagger_{\overline{\mu}_i}(t_i)\,\cdots|\Phi_0^{\rm n}\rangle\ . \qquad (68)
\end{aligned}
$$

Here we used $c_{\overline{\overline{\nu}}} = -c_\nu$. The summation indices (μ_i, ν_i) can be replaced by $(\overline{\nu}_i, \overline{\mu}_i)$. Thus Eq. (67) reads

$$
\begin{aligned}
&\begin{pmatrix} iG^{11}_{\nu\mu}(t) & iG^{12}_{\nu\overline{\mu}}(t) \\ iG^{21}_{\overline{\nu}\mu}(t) & iG^{22}_{\overline{\nu}\overline{\mu}}(t) \end{pmatrix} \\
= \quad & \sum_{m=0}^{\infty}\left(\frac{-i}{\hbar}\right)^m \frac{1}{m!}\int_{-\infty}^{\infty}dt_1\cdots\int_{-\infty}^{\infty}dt_m\frac{1}{2^m} \\
& \times\sum_{l_1m_1}\kappa_{l_1}\sum_{\nu_1\mu_1}(\langle\mu_1|F^\dagger_{l_1m_1}|\nu_1\rangle + \langle\overline{\nu}_1|F^\dagger_{l_1m_1}|\overline{\mu}_1\rangle) \\
& \times\cdots \\
& \times\sum_{l_mm_m}\kappa_{l_m}\sum_{\nu_m\mu_m}(\langle\mu_m|F^\dagger_{l_mm_m}|\nu_m\rangle + \langle\overline{\nu}_m|F^\dagger_{l_mm_m}|\overline{\mu}_m\rangle) \\
& \times\langle\Phi_0^{\rm ph}|[\hat{\alpha}_{l_1m_1}(t_1)\hat{\alpha}_{l_2m_2}(t_2)\quad\cdots\quad\hat{\alpha}_{l_mm_m}(t_m) \\
& \quad +\text{all other possible full contractions }]|\Phi_0^{\rm ph}\rangle \\
& \times\langle\Phi_0^{\rm n}|[\Psi^\dagger_{\mu_1}(t_1)\,\tau_3\Psi_{\nu_1}(t_1)\quad\cdots\quad\Psi^\dagger_{\mu_m}(t_m)\ \ \tau_3\Psi_{\nu_m}(t_m)\Psi_\nu(t)\,\Psi^\dagger_\mu \\
& \quad +\text{ all other possible full contractions between }\Psi\text{ and }\Psi^\dagger]|\Phi_0^{\rm n}\rangle_{\rm conn}\ . \qquad (69)
\end{aligned}
$$

Now let us introduce a permutation $\mathcal{P}$ of the integers (1,2, $\cdots$ m,0) $\rightarrow$ (p(1),p(2), $\cdots$, $p(m)$, p(0)) in order to express the contractions explicitly:

$$
\begin{aligned}
\mathcal{P} &= \begin{pmatrix} 1 & 2 & \cdots & m & 0 \\ p(1) & p(2) & \cdots & p(m) & p(0) \end{pmatrix} \\
&= \begin{pmatrix} X(1) & X(2) & \cdots & X(m_1) \\ X(2) & X(3) & \cdots & X(1) \end{pmatrix} \\
&\quad\times\begin{pmatrix} X(m_1+1) & X(m_1+2) & \cdots & X(m_2) \\ X(m_1+2) & X(m_1+3) & \cdots & X(m_1+1) \end{pmatrix}\cdots \\
&\quad\times\begin{pmatrix} X(m_{P-1}+1) & X(m_{P-1}+2) & \cdots & X(m_P) \\ X(m_{P-1}+2) & X(m_{P-1}+3) & \cdots & X(m_{P-1}+1) \end{pmatrix}\ . \qquad (70)
\end{aligned}
$$

Here the decomposition of $\mathcal{P}$ into the product of the cyclic permutations can be obtained as follows:

i) Choose an arbitrary integer i $\in$ { 1,2, $\cdots$ m,0 } and define $X(1) = i$.

ii) Put $X(2) = p(X(1))$, $X(3) = p(X(2))$, $\cdots$.

iii) If $p(X(m_1)) = X(1)$, then choose an integer j which is not yet used, and put $X(m_1 + 1) = j$.

iv) Repeat the procedure.

This is a well-known theorem in the permutation group theory. One of the cyclic permutations includes 0. We put

$$X(m_{N-1} + 1) = 0 \ , \tag{71}$$

for later convenience. By applying the permutation, the summation of all possible full contractions between Ψ and $\Psi^\dagger$ can be written as

$$\begin{aligned}
&\langle \Phi_0^{\rm n}| [\underbrace{\Psi^\dagger_{\mu_1}(t_1)\tau_3\Psi_{\nu_1}(t_1)}\ \cdots\ \underbrace{\Psi^\dagger_{\mu_m}(t_m)\,\tau_3\Psi_{\nu_m}(t_m)\,\Psi_\nu(t)\,\Psi^\dagger_\mu} \\
&\quad + \text{all other possible full contractions between } \Psi \text{ and } \Psi^\dagger] |\Phi_0^{\rm n}\rangle_{\rm conn} \\
&= \sum_{\mathcal{P}_{\rm conn}} A_1 A_2 \cdots A_P \ ,
\end{aligned} \tag{72}$$

where

$$\begin{aligned}
A_{i+1} \ = \ & -{\rm Tr} \left[\tau_3 \begin{pmatrix} iG_0^{11}\nu_{X(m_i+1)}\,\mu_{X(m_i+2)} & iG_0^{12}\nu_{X(m_i+1)}\,\overline{\mu}_{X(m_i+2)} \\ iG_0^{21}\overline{\nu}_{X(m_i+1)}\,\mu_{X(m_i+2)} & iG_0^{22}\overline{\nu}_{X(m_i+1)}\,\overline{\mu}_{X(m_i+2)} \end{pmatrix}_{(t_{X(m_i+1)},\, t_{X(m_i+2)})} \right. \\
& \times \tau_3 \begin{pmatrix} iG_0^{11}\nu_{X(m_i+2)}\,\mu_{X(m_i+3)} & iG_0^{12}\nu_{X(m_i+2)}\,\overline{\mu}_{X(m_i+3)} \\ iG_0^{21}\overline{\nu}_{X(m_i+2)}\,\mu_{X(m_i+3)} & iG_0^{22}\overline{\nu}_{X(m_i+2)}\,\overline{\mu}_{X(m_i+3)} \end{pmatrix}_{(t_{X(m_i+2)},\, t_{X(m_i+3)})} \\
& \times \cdots \\
& \times \tau_3 \begin{pmatrix} iG_0^{11}\nu_{X(m_{i+1}-1)}\,\mu_{X(m_{i+1})} & iG_0^{12}\nu_{X(m_{i+1}-1)}\,\overline{\mu}_{X(m_{i+1})} \\ iG_0^{21}\overline{\nu}_{X(m_{i+1}-1)}\,\mu_{X(m_{i+1})} & iG_0^{22}\overline{\nu}_{X(m_{i+1}-1)}\,\overline{\mu}_{X(m_{i+1})} \end{pmatrix}_{(t_{X(m_{i+1}-1)},\, t_{X(m_{i+1})})} \\
& \left. \times \ \tau_3 \begin{pmatrix} iG_0^{11}\nu_{X(m_{i+1})}\,\mu_{X(m_i+1)} & iG_0^{12}\nu_{X(m_{i+1})}\,\overline{\mu}_{X(m_i+1)} \\ iG_0^{21}\overline{\nu}_{X(m_{i+1})}\,\mu_{X(m_i+1)} & iG_0^{22}\overline{\nu}_{X(m_{i+1})}\,\overline{\mu}_{X(m_i+1)} \end{pmatrix}_{(t_{X(m_{i+1})},\, t_{X(m_i+1)})} \right] ,
\end{aligned} \tag{73}$$

where it is assumed that A_{i+1} does not have the indices $\nu \equiv \nu_0$ and $\mu \equiv \mu_0$. In the derivation we have used

$$\begin{aligned}
\underbrace{\Psi_{\nu_i}(t_i)\Psi^\dagger_{\mu_j}}(t_j) \quad &= \quad \begin{pmatrix} iG_0^{11}{}_{\nu_i\mu_j}(t_i,t_j) & iG_0^{12}{}_{\nu_i\overline{\mu}_j}(t_i,t_j) \\ iG_0^{21}{}_{\overline{\nu}_i\mu_j}(t_i,t_j) & iG_0^{22}{}_{\overline{\nu}_i\overline{\mu}_j}(t_i,t_j) \end{pmatrix} \\
&\equiv \quad \begin{pmatrix} iG_0^{11}{}_{\nu_i\mu_j} & iG_0^{12}{}_{\nu_i\overline{\mu}_j} \\ iG_0^{21}{}_{\overline{\nu}_i\mu_j} & iG_0^{22}{}_{\overline{\nu}_i\overline{\mu}_j} \end{pmatrix}_{(t_i,t_j)} ,
\end{aligned} \tag{74}$$

and

$$(a,b)\begin{pmatrix} c \\ d \end{pmatrix} = \mathrm{Tr}\begin{pmatrix} c \\ d \end{pmatrix}(a,b)\ . \tag{75}$$

The product of G_0 including the suffices ν and μ is a 2 by 2 matrix:

$$\begin{aligned} A_N \ = \ & \begin{pmatrix} iG_0^{11}\nu\,\mu_{X(m_{N-1}+2)} & iG_0^{12}\nu\,\overline{\mu}_{X(m_{N-1}+2)} \\ iG_0^{21}\overline{\nu}\,\mu_{X(m_{N-1}+2)} & iG_0^{22}\overline{\nu}\,\overline{\mu}_{X(m_{N-1}+2)} \end{pmatrix}_{(t,\,t_{X(m_{N-1}+2)})} \\ \times\tau_3 & \begin{pmatrix} iG_0^{11}\nu_{X(m_{N-1}+2)}\,\mu_{X(m_{N-1}+3)} & iG_0^{12}\nu_{X(m_{N-1}+2)}\,\overline{\mu}_{X(m_{N-1}+3)} \\ iG_0^{21}\overline{\nu}_{X(m_{N-1}+2)}\,\mu_{X(m_{N-1}+3)} & iG_0^{22}\overline{\nu}_{X(m_{N-1}+2)}\,\overline{\mu}_{X(m_{N-1}+3)} \end{pmatrix}_{(t_{X(m_{N-1}+2)},\,t_{X(m_{N-1}+3)})} \\ & \times\cdots \\ & \times\tau_3 \begin{pmatrix} iG_0^{11}\nu_{X(m_N-1)}\,\mu_{X(m_N)} & iG_0^{12}\nu_{X(m_N-1)}\,\overline{\mu}_{X(m_N)} \\ iG_0^{21}\overline{\nu}_{X(m_N-1)}\,\mu_{X(m_N)} & iG_0^{22}\overline{\nu}_{X(m_N-1)}\,\overline{\mu}_{X(m_N)} \end{pmatrix}_{(t_{X(m_N-1)},\,t_{X(m_N)})} \\ & \times\tau_3 \begin{pmatrix} iG_0^{11}\nu_{X(m_N)}\,\mu & iG_0^{12}\nu_{X(m_N)}\,\overline{\mu} \\ iG_0^{21}\overline{\nu}_{X(m_N)}\,\mu & iG_0^{22}\overline{\nu}_{X(m_N)}\,\overline{\mu} \end{pmatrix}_{(t_{X(m_N)},\,0)} , \end{aligned} \tag{76}$$

with

$$\nu = \nu_0 = \nu_{X(m_{N-1}+1)}\ , \tag{77}$$

$$\mu = \mu_0 = \mu_{X(m_{N-1}+1)}\ . \tag{78}$$

For m in Eq. (69) there are $m!$ identical terms which are obtained to each other by an exchange of the set of the summation indices and an integral variable (μ_i, ν_i, l_i, m_i, t_i) $\leftrightarrow$ (μ_j, ν_j, l_j, m_j, t_j). They are called topologically equivalent, otherwise the terms are called topologically distinct. One of the topologically equivalent terms has always

$$\begin{aligned} & \hat{\alpha}_{\underbrace{l_1 m_1}}(t_1)\,\hat{\alpha}_{\underbrace{l_2 m_2}}(t_2)\,\hat{\alpha}_{\underbrace{l_3 m_3}}(t_3)\,\hat{\alpha}_{\underbrace{l_4 m_4}}(t_4) \quad \cdots\hat{\alpha}_{\underbrace{l_{m-1} m_{m-1}}}(t_{m-1})\,\hat{\alpha}_{\underbrace{l_m m_m}}(t_m) \\ & \quad = (\alpha_{l_1})_0\ (\alpha_{l_2})_0\ iD^0_{l_1 m_1, l_2 m_2}(t_1,t_2)\ (\alpha_{l_3})_0\ (\alpha_{l_4})_0\ iD^0_{l_3 m_3, l_4 m_4}(t_3,t_4)\cdots \\ & \qquad \times (\alpha_{l_{m-1}})_0\ (\alpha_{l_m})_0\ iD^0_{l_{m-1} m_{m-1}, l_m m_m}(t_{m-1},t_m)\ , \end{aligned} \tag{79}$$

where $iD^0_{l_1 m_1, l_2 m_2}(t_1,t_2)$ is the unperturbed phonon Green function. Thus Eq. (69) becomes

$$\begin{aligned} & \begin{pmatrix} iG^{11}_{\nu\mu}(t) & iG^{12}_{\nu\overline{\mu}}(t) \\ iG^{21}_{\overline{\nu}\mu}(t) & iG^{22}_{\overline{\nu}\,\overline{\mu}}(t) \end{pmatrix} \\ = \ & \sum_{m=0,2,\cdots}^{\infty}\left(\frac{-i}{\hbar}\right)^m \int_{-\infty}^{\infty} dt_1\cdots\int_{-\infty}^{\infty} dt_m \\ & \times \sum_{l_1 m_1}(\alpha_{l_1})_0\ \kappa_{l_1} \sum_{\nu_1\mu_1}\langle\mu_1|F^{\dagger}_{l_1 m_1}|\nu_1\rangle\cdots\sum_{l_m m_m}(\alpha_{l_m})_0\ \kappa_{l_m}\sum_{\nu_m\mu_m}\langle\mu_m|F^{\dagger}_{l_m m_m}|\nu_m\rangle \\ & \times \sum_{\substack{\mathcal{P}_{\mathrm{conn}} \\ \text{topologically distinct}}} iD^0_{l_1 m_1, l_2 m_2}(t_1,t_2)\,iD^0_{l_3 m_3, l_4 m_4}(t_3,t_4)\cdots iD^0_{l_{m-1} m_{m-1}, l_m m_m}(t_{m-1},t_m) \\ & \times A_1 A_2\cdots A_P\ . \end{aligned} \tag{80}$$

One may put the unperturbed Green functions to be diagonal:

$$iG_0^{11}{}_{\nu\mu}(t,t') = iG_0^{11}{}_{\nu}(t,t')\delta_{\mu\nu} \ , \tag{81}$$
$$iG_0^{22}{}_{\overline{\nu}\,\overline{\mu}}(t,t') = iG_0^{22}{}_{\overline{\nu}}(t,t')\delta_{\mu\nu} \ , \tag{82}$$
$$iG_0^{12}{}_{\nu\,\overline{\mu}}(t,t') = iG_0^{12}{}_{\nu\,\overline{\nu}}(t,t')\delta_{\mu\nu} \ , \tag{83}$$
$$iG_0^{21}{}_{\overline{\nu}\,\mu}(t,t') = iG_0^{21}{}_{\overline{\nu}\,\nu}(t,t')\delta_{\mu\nu} \ , \tag{84}$$
$$iD^0_{l_im_i,l_{i+1}m_{i+1}}(t_i,t_{i+1}) = iD^0_{l_im_i}(t_i,t_{i+1})\delta_{l_il_{i+1}}\delta_{m_i\,-m_{i+1}} \ . \tag{85}$$

That is, we can put

$$\mu_{X(i+1)} = \nu_{X(i)} \ , \tag{86}$$

in Eqs. (73) and (76). Consequently the final form of the perturbed Green function in the time representation is given by

$$\begin{aligned}
&\begin{pmatrix} iG^{11}_{\nu\mu}(t) & iG^{12}_{\nu\overline{\mu}}(t) \\ iG^{21}_{\overline{\nu}\mu}(t) & iG^{22}_{\overline{\nu}\,\overline{\mu}}(t) \end{pmatrix} \\
= \quad & \sum_{m=0,2,\cdots}^{\infty} \left(\frac{-i}{\hbar}\right)^m \int_{-\infty}^{\infty} dt_1 \cdots \int_{-\infty}^{\infty} dt_m \\
& \times \sum_{l_1m_1} \sum_{l_2m_2} \cdots \sum_{l_{m-1}m_{m-1}} \sum_{\nu_1\nu_2\cdots\nu_m}{}' \\
& \times (\alpha_{l_1})_0 \ \kappa_{l_1} \langle \nu_{\overline{p}(1)} | F^\dagger_{l_1m_1} | \nu_1 \rangle \ (\alpha_{l_1})_0 \ \kappa_{l_1} \langle \nu_{\overline{p}(2)} | F^\dagger_{l_1\,-m_1} | \nu_2 \rangle \\
& \times (\alpha_{l_3})_0 \ \kappa_{l_3} \langle \nu_{\overline{p}(3)} | F^\dagger_{l_3m_3} | \nu_3 \rangle \ (\alpha_{l_3})_0 \ \kappa_{l_3} \langle \nu_{\overline{p}(4)} | F^\dagger_{l_3\,-m_3} | \nu_4 \rangle \\
& \times \cdots \\
& \times (\alpha_{l_{m-1}})_0 \ \kappa_{l_{m-1}} \langle \nu_{\overline{p}(m-1)} | F^\dagger_{l_{m-1}m_{m-1}} | \nu_{m-1} \rangle \ (\alpha_{l_{m-1}})_0 \ \kappa_{l_{m-1}} \langle \nu_{\overline{p}(m)} | F^\dagger_{l_{m-1}\,-m_{m-1}} | \nu_m \rangle \\
& \times \sum_{\substack{\mathcal{P}_{\rm conn} \\ \text{topologically distinct}}} iD^0_{l_1m_1}(t_1,t_2)\, iD^0_{l_3m_3}(t_3,t_4) \cdots iD^0_{l_{m-1}m_{m-1}}(t_{m-1},t_m) \\
& \times A_1 A_2 \cdots A_P \ ,
\end{aligned} \tag{87}$$

where $\langle \nu_{\overline{p}(X(m_{N-1}+1))}| = \langle \nu_{X(m_N)}|$ is replaced by $\langle \mu|$, and $|\nu_{X(m_{N-1}+1)}\rangle = |\nu_0\rangle$ is replaced by $|\nu\rangle$ in the matrix elements of $F^\dagger_{lm}$. $\sum'_{\nu_1\nu_2\cdots\nu_m}$ does not contain $\nu_{X(m_N)}$. $\overline{p}(i)$ denotes $p^{-1}(i)$. A_i takes the form

$$\begin{aligned}
& A_{i\neq N} \\
= \quad & -\mathrm{Tr} \left[\tau_3 \begin{pmatrix} iG_0^{11}\nu_{X(m_{i-1}+1)} & iG_0^{12}{}_{\nu_{X(m_{i-1}+1)}\,\overline{\nu}_{X(m_{i-1}+1)}} \\ iG_0^{21}{}_{\overline{\nu}_{X(m_{i-1}+1)}\,\nu_{X(m_{i-1}+1)}} & iG_0^{22}\overline{\nu}_{X(m_{i-1}+1)} \end{pmatrix}_{(t_{X(m_{i-1}+1)},\, t_{X(m_{i-1}+2)})} \right. \\
& \times \tau_3 \begin{pmatrix} iG_0^{11}\nu_{X(m_{i-1}+2)} & iG_0^{12}{}_{\nu_{X(m_{i-1}+2)}\,\overline{\nu}_{X(m_{i-1}+2)}} \\ iG_0^{21}{}_{\overline{\nu}_{X(m_{i-1}+2)}\,\nu_{X(m_{i-1}+2)}} & iG_0^{22}\overline{\nu}_{X(m_{i-1}+2)} \end{pmatrix}_{(t_{X(m_{i-1}+2)},\, t_{X(m_{i-1}+3)})} \\
& \times \cdots \\
& \left. \times \tau_3 \begin{pmatrix} iG_0^{11}\nu_{X(m_i)} & iG_0^{12}{}_{\nu_{X(m_i)}\,\overline{\nu}_{X(m_i)}} \\ iG_0^{21}{}_{\overline{\nu}_{X(m_i)}\,\nu_{X(m_i)}} & iG_0^{22}\overline{\nu}_{X(m_i)} \end{pmatrix}_{(t_{X(m_i)},\, t_{X(m_{i-1}+1)})} \right] ,
\end{aligned} \tag{88}$$

$$
\begin{aligned}
A_N &= \left(\begin{array}{cc} iG_0^{11}\nu & iG_0^{12}\nu\,\overline{\nu} \\ iG_0^{21}\overline{\nu}\,\nu & iG_0^{22}\overline{\nu} \end{array} \right)_{(t,\, t_{X(m_{N-1}+2)})} \\
&\times\tau_3 \left(\begin{array}{cc} iG_0^{11}\nu_{X(m_{N-1}+2)} & iG_0^{12}\nu_{X(m_{N-1}+2)}\,\overline{\nu}_{X(m_{N-1}+2)} \\ iG_0^{21}\overline{\nu}_{X(m_{N-1}+2)}\,\nu_{X(m_{N-1}+2)} & iG_0^{22}\overline{\nu}_{X(m_{N-1}+2)} \end{array} \right)_{(t_{X(m_{N-1}+2)},\, t_{X(m_{N-1}+3)})} \\
&\quad\times\cdots \\
&\quad\times\tau_3 \left(\begin{array}{cc} iG_0^{11}\nu_{X(m_N-1)} & iG_0^{12}\nu_{X(m_N-1)}\,\overline{\nu}_{X(m_N-1)} \\ iG_0^{21}\overline{\nu}_{X(m_N-1)}\,\nu_{X(m_N-1)} & iG_0^{22}\overline{\nu}_{X(m_N-1)} \end{array} \right)_{(t_{X(m_N-1)},\, t_{X(m_N)})} \\
&\quad\times\tau_3 \left(\begin{array}{cc} iG_0^{11}\mu & iG_0^{12}\mu\,\overline{\mu} \\ iG_0^{21}\overline{\mu}\,\mu & iG_0^{22}\overline{\mu} \end{array} \right)_{(t_{X(m_N)},\, 0)} .
\end{aligned}
\tag{89}
$$

The perturbed Green function in Lehmann representation is obtained

$$
\begin{aligned}
&\frac{1}{\hbar}\left(\begin{array}{cc} iG^{11}_{\nu\mu}(\omega) & iG^{12}_{\nu\overline{\mu}}(\omega) \\ iG^{21}_{\overline{\nu}\mu}(\omega) & iG^{22}_{\overline{\nu}\,\overline{\mu}}(\omega) \end{array} \right) \\
&= \lim_{\delta\to+0}\frac{1}{\hbar}\int_{-\infty}^{\infty} dt\, e^{i(\omega+i(2\theta(t)-1)\delta)t/\hbar} \left(\begin{array}{cc} iG^{11}_{\nu\mu}(t) & iG^{12}_{\nu\overline{\mu}}(t) \\ iG^{21}_{\overline{\nu}\mu}(t) & iG^{22}_{\overline{\nu}\,\overline{\mu}}(t) \end{array} \right) \\
&= \sum_{m=0,2,\cdots}^{\infty}\left(\frac{-i}{\hbar}\right)^m \sum_{\substack{\mathcal{P}_{\rm conn} \\ \text{topologically distinct}}} \int_{-\infty}^{\infty}\frac{dw_1}{2\pi}\int_{-\infty}^{\infty}\frac{dw_2}{2\pi}\cdots\int_{-\infty}^{\infty}\frac{dw_m}{2\pi} \\
&\quad\times\sum_{l_1m_1}\sum_{l_3m_3}\cdots\sum_{l_{m-1}m_{m-1}}\sum_{1,2,\cdots,m}{}' \\
&\quad\times(\alpha_{l_1})_0\,\kappa_{l_1}\langle\overline{p}(1)|F^\dagger_{l_1m_1}|1\rangle\,(\alpha_{l_1})_0\,\kappa_{l_1}\langle\overline{p}(2)|F^\dagger_{l_1\,-m_1}|2\rangle \\
&\quad\times(\alpha_{l_3})_0\,\kappa_{l_3}\langle\overline{p}(3)|F^\dagger_{l_3m_3}|3\rangle\,(\alpha_{l_3})_0\,\kappa_{l_3}\langle\overline{p}(4)|F^\dagger_{l_3\,-m_3}|4\rangle\,\cdots \\
&\quad\times(\alpha_{l_{m-1}})_0\,\kappa_{l_{m-1}}\langle\overline{p}(m-1)|F^\dagger_{l_{m-1}m_{m-1}}|m-1\rangle\,(\alpha_{l_{m-1}})_0\,\kappa_{l_{m-1}}\langle\overline{p}(m)|F^\dagger_{l_{m-1}\,-m_{m-1}}|m\rangle \\
&\quad\times\frac{i}{\hbar}D^0_{l_1m_1}(-w_1+w_{\overline{p}(1)})\frac{i}{\hbar}D^0_{l_3m_3}(-w_3+w_{\overline{p}(3)})\cdots\frac{i}{\hbar}D^0_{l_{m-1}m_{m-1}}(-w_{m-1}+w_{\overline{p}(m-1)}) \\
&\quad\times\mathcal{A}_1\mathcal{A}_2\cdots\mathcal{A}_P \\
&\quad\times 2\pi\hbar^2\,\delta(w_1+w_2-w_{\overline{p}(1)}-w_{\overline{p}(2)})\,2\pi\hbar^2\,\delta(w_3+w_4-w_{\overline{p}(3)}-w_{\overline{p}(4)})\cdots \\
&\quad\times 2\pi\hbar^2\,\delta(w_{m-1}+w_m-w_{\overline{p}(m-1)}-w_{\overline{p}(m)})\ .
\end{aligned}
\tag{90}
$$

We have used an abbreviation $|i\rangle = |\nu_i\rangle$. As in the time-representation (87), $\langle\overline{p}(X(m_{N-1}+1))| = \langle X_{m_N}|$ is replaced by $\langle\mu|$, and $|X(m_{N-1}+1)\rangle = |0\rangle$ is replaced by $|\nu\rangle$ in the matrix elements of $F^\dagger_{lm}$. $\sum'_{1,2,\cdots,m}$ does not contain $X(m_N)$. Note $w_0=\omega$. $\mathcal{A}$ can be written

$$
\begin{aligned}
\mathcal{A}_{i\neq N} &= -\mathrm{Tr}\left[\,\tau_3\frac{i}{\hbar}G^0_{X(m_{i-1}+1)}(w_{X(m_{i-1}+1)})\tau_3\frac{i}{\hbar}G^0_{X(m_{i-1}+2)}(w_{X(m_{i-1}+2)})\right. \\
&\quad\left.\times\cdots\tau_3\frac{i}{\hbar}G^0_{X(m_i)}(w_{X(m_i)})\,\right] ,
\end{aligned}
\tag{91}
$$

where

$$G_i^0(w) \equiv \begin{pmatrix} {G_0^{11}}_{\nu_i}(w) & {G_0^{12}}_{\nu_i\overline{\nu}_i}(w) \\ {G_0^{21}}_{\overline{\nu}_i\nu_i}(w) & {G_0^{22}}_{\overline{\nu}_i}(w) \end{pmatrix} . \tag{92}$$

For $i = N$,

$$\begin{aligned} \mathcal{A}_N &= \frac{i}{\hbar} G_0^0(w_0)\tau_3 \frac{i}{\hbar} G^0_{X(m_{N-1}+2)}(w_{X(m_{N-1}+2)}) \\ &\quad \times \cdots \tau_3 \frac{i}{\hbar} G^0_{X(m_N)}(w_{X(m_N)}) , \end{aligned} \tag{93}$$

where

$$G^0_{X(m_{N-1}+1)}(w_{X(m_{N-1}+1)}) = G_0^0(w_0) \equiv G_\nu^0(\omega) , \tag{94}$$

$$G^0_{X(m_N)}(w_{X(m_N)}) \equiv G_\mu^0(\omega) . \tag{95}$$

If $N = 1$, one may put $m_{N-1} = 0$. Now the diagram rule for $(1/\hbar)G_\mu(\omega)$ is clear from Eqs. (90) – (95):

i) Draw connected topologically-distinct diagrams with the unperturbed nucleon Green functions, phonon Green functions and the interaction points, and assign $(1/\hbar)G_\mu^0(w)$, $(i/\hbar)D_{lm}^0(w)$, $(\alpha_l)_0\,\kappa_l\langle\nu|F_{lm}^\dagger|\mu\rangle$ for emitting a phonon with (lm) and $(\alpha_l)_0\,\kappa_l\langle\nu|F_{l\,-m}^\dagger|\mu\rangle$ for absorbing a phonon (lm), respectively, with adequate suffices μ_1, l_1m_1 etc. The definition of "connected" is that any part of the diagram is connected to the other part by either nucleon or phonon Green function. Assign intermediate energies in such a way that the interaction points conserve the energy.

ii) Make products of the nucleon Green functions in the order indicated by the diagram putting τ_3 at the connecting points of the nucleon Green functions.

iii) If the product is a closed loop, take $-$Tr of the product.

iv) Take summations with respect to the intermediate single-particle states, lm and the integral $\int_{-\infty}^{\infty} d\omega_i/2\pi$ with respect to the intermediate energies ω_i's.

ii) and iii) are the points different from the usual rule without the anomalous Green function.

A simple example of diagram is shown in Fig. A-1.

Using the diagram rule i) – iv), one can obtain the equation

$$\begin{aligned} \frac{1}{\hbar} G_{\nu\mu}(\omega) &= \int \frac{d\omega_2}{2\pi} \sum_{lm} \sum_{\nu_2} \frac{1}{\hbar} G_\nu^0(\omega)\tau_3 \frac{1}{\hbar} G_{\nu_2}^0(\omega_2)\tau_3 \frac{1}{\hbar} G_\mu^0(\omega) \\ &\quad \times (\alpha_l)_0\,\kappa_l\langle\nu_2|F_{lm}^\dagger|\mu\rangle (\alpha_l)_0\,\kappa_l\langle\nu|F_{l\,-m}^\dagger|\nu_2\rangle \\ &\quad \times \frac{i}{\hbar} D_{lm}^0(\omega - \omega_2) , \end{aligned} \tag{96}$$

The self-energy is defined by removing the entering and exiting nucleon Green function from the diagram.

We have two comments on the above derivation. The final result of the diagram rule is identical to that of the original formulation [43]. The difference is that we

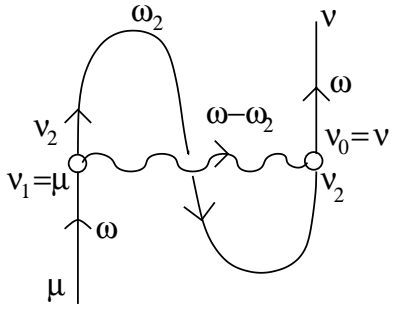

Figure A-1. An example of diagram.

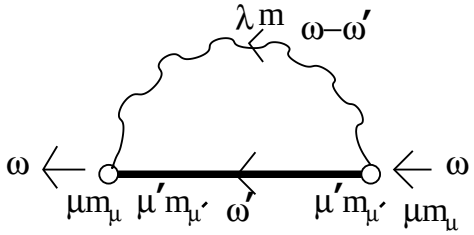

Figure B-1. A self-energy.

have $\Psi_\mu(\cdots)\Psi_\nu \neq 0$. If an extension of the Nambu-Gor'kov formulation is made for a two-body force dependent on the spin, derivation of the diagram rule would be more complicated. Second, the diagram rule derived here is mathematically equivalent to the ways proposed in [39, 38]. Migdal et al. do not use the 2×2 matrix form.

Appendix B – spherically symmetric case –

Let us consider the self-energy given by Fig. B-1 under the spherical symmetry of the system.

Using the diagram rule derived in Appendix A, we can write

$$\begin{aligned}\hbar\Sigma_\mu(\omega) &= \int_{-\infty}^{\infty}\frac{d\omega'}{2\pi}\sum_{\lambda m}\sum_{\mu' m_{\mu'}}\tau_3\frac{1}{\hbar}G_{\mu'}(\omega')\tau_3 \\ &\quad\times(\alpha_\lambda)_0\,\kappa_\lambda\langle\mu' m_{\mu'}|F^\dagger_{\lambda m}|\mu m_\mu\rangle(\alpha_\lambda)_0\,\kappa_\lambda\langle\mu m_\mu|F^\dagger_{\lambda -m}|\mu' m_{\mu'}\rangle\frac{i}{\hbar}D^0_{\lambda m}(\omega-\omega')\ .\end{aligned} \tag{97}$$

For the notations used, see Appendix A. Note that μ in Appendix A corresponds to $(\mu m_\mu) = (nljm)_\mu$ here. m is the z-component of the multipolarity λ, which is assumed to have only one phonon mode in this appendix for simplicity. The vertex matrix element can be written

$$(\alpha_\lambda)_0\,\kappa_\lambda\langle\mu m_\mu|F_{\lambda m}|\mu' m_{\mu'}\rangle = -\sqrt{\frac{\hbar}{2\Omega_\lambda B_\lambda}}(-)^{j_\mu - m_\mu}\begin{pmatrix} j_\mu & \lambda & j_{\mu'} \\ -m_\mu & m & m_{\mu'}\end{pmatrix}\langle\mu||R_0\frac{dU(r)}{dr}Y_\lambda||\mu'\rangle\ , \tag{98}$$

It is possible to make the vertex matrix elements real.

For the unperturbed phonon Green function, we have

$$iD^0_{\lambda m}(t) \stackrel{d}{=} \langle\Phi_{\rm ph}|{\rm T}[(c^\dagger_{\lambda m}(t)+c_{\overline{\lambda m}}(t))(c^\dagger_{\lambda\,-m}+c_{\overline{\lambda\,-m}})]|\Phi_{\rm ph}\rangle \tag{99}$$

$$= \begin{cases} (-)^m\, e^{-i\Omega_\lambda t}, & t>0 \\ (-)^m\, e^{i\Omega_\lambda t}, & t<0 \end{cases} , \tag{100}$$

where the phonon creation and annihilation operators have relations

$$c^\dagger_{\lambda m}(t) = c^\dagger_{\lambda m} e^{i\Omega_\lambda t} , \tag{101}$$

$$c_{\overline{\lambda m}} = (-)^m\, c_{\lambda\,-m} . \tag{102}$$

$|\Phi_{\rm ph}\rangle$ is a phonon vacuum state. The Green function in Lehmann representation is given by

$$iD^0_{\lambda m}(\omega) \stackrel{d}{=} \lim_{\delta\to+0}\int_{-\infty}^{\infty} dt\, e^{i\omega t/\hbar}\, iD^0_{\lambda m}(t) e^{-\delta(2\theta(t)-1)t/\hbar}$$

$$= (-)^m\, iD^0_\lambda(\omega) , \tag{103}$$

$$iD^0_\lambda(\omega) = \frac{i\hbar}{\omega-\hbar\Omega_\lambda+i\delta\hbar} - \frac{i\hbar}{\omega+\hbar\Omega_\lambda-i\delta\hbar} . \tag{104}$$

Inserting Eqs. (98) and (103) to Eq. (97), we obtain

$$\hbar\Sigma_\mu(\omega) = \int_{-\infty}^{\infty}\frac{d\omega'}{2\pi}\sum_\lambda\sum_{\mu'}\tau_3\frac{1}{\hbar}G_{\mu'}(\omega')\tau_3$$

$$\times\frac{\hbar}{2\Omega_\lambda B_\lambda}\frac{1}{2j_\mu+1}\left|\langle\mu||R_0\frac{dU(r)}{dr}Y_\lambda||\mu'\rangle\right|^2\frac{i}{\hbar}D^0_\lambda(\omega-\omega') . \tag{105}$$

Appendix C – general form of particle Green function –

The particle Green functions in the time representation are defined

$$G^{11}_\mu(t) = -i\langle\Psi_0|{\rm T}[c_{\mu m_\mu}(t)\, c^\dagger_{\mu m_\mu}]|\Psi_0\rangle, \tag{106}$$

$$G^{22}_\mu(t) = -i\langle\Psi_0|{\rm T}[c^\dagger_{\overline{\mu m_\mu}}(t)\, c_{\overline{\mu m_\mu}}]|\Psi_0\rangle, \tag{107}$$

where $|\Psi_0\rangle$ is an N-particle ground state with N being an even number. The time-dependent creation operator of the single-particle is defined by

$$c^\dagger_{\mu m_\mu}(t) = e^{iH't/\hbar}c^\dagger_{\mu m_\mu}e^{-iH't/\hbar} ,$$

$$H' = H - \varepsilon_F\hat{N} .$$

H is the many-body Hamiltonian. ε_F is the Fermi level, and $\hat{N}$ denotes the particle-number operator. $\overline{(\mu m_\mu)}$ indicates the time-reversed state of (μm_μ). Since $|\Psi_0\rangle$ is spherically symmetric, the Green function is a scalar. Eqs. (106) and (107) yield

i) t $>$ 0

$$
\begin{aligned}
G_{\mu}^{11}(t) &= -i\langle\Psi_0|c_{\mu m_\mu}(t)\, c_{\mu m_\mu}^{\dagger}|\Psi_0\rangle \\
&= -i\sum_i e^{i(E_0-E_i)t/\hbar}\langle\Psi_0|c_{\mu m_\mu}|\Psi_i\rangle\langle\Psi_i|c_{\mu m_\mu}^{\dagger}|\Psi_0\rangle \ , \qquad (108)\\
G_{\mu}^{22}(t) &= -i\langle\Psi_0|c_{\overline{\mu m_\mu}}^{\dagger}(t)\, c_{\overline{\mu m_\mu}}|\Psi_0\rangle \\
&= -i\sum_i e^{i(E_0-E_i)t/\hbar}\langle\Psi_0|c_{\overline{\mu m_\mu}}^{\dagger}|\Psi_i\rangle\langle\Psi_i|c_{\overline{\mu m_\mu}}|\Psi_0\rangle \ , \qquad (109)
\end{aligned}
$$

ii) t $<$ 0

$$
\begin{aligned}
G_{\mu}^{11}(t) &= -i\langle\Psi_0|(-)c_{\mu m_\mu}^{\dagger}\, c_{\mu m_\mu}(t)|\Psi_0\rangle \\
&= i\sum_i e^{i(E_i-E_0)t/\hbar}\langle\Psi_0|c_{\mu m_\mu}^{\dagger}|\Psi_i\rangle\langle\Psi_i|c_{\mu m_\mu}|\Psi_0\rangle \ , \qquad (110)\\
G_{\mu}^{22}(t) &= -i\langle\Psi_0|(-)c_{\overline{\mu m_\mu}}\, c_{\overline{\mu m_\mu}}^{\dagger}(t)|\Psi_0\rangle \\
&= i\sum_i e^{i(E_i-E_0)t/\hbar}\langle\Psi_0|c_{\overline{\mu m_\mu}}|\Psi_i\rangle\langle\Psi_i|c_{\overline{\mu m_\mu}}^{\dagger}|\Psi_0\rangle \ . \qquad (111)
\end{aligned}
$$

E_0 is the ground-state eigenenergy of H'. $\{\Psi_i\}$ indicates a complete set of a many-body space which consists of $N\pm 1$,$N\pm 3\cdots$-particle states. E_i is the eigenenergy of $|\Psi_i\rangle$ for H'.

The Green functions in Lehmann representation read

$$
\begin{aligned}
G_{\mu}^{11}(\omega) &\stackrel{d}{=} \lim_{\eta\to+0}\int_{-\infty}^{\infty} dt\, e^{i\omega t/\hbar}\, G_{\mu}^{11}(t)\, e^{-(2\theta(t)-1)\eta t} \\
&= \sum_i \frac{\left|\langle\Psi_0|c_{\mu m_\mu}|\Psi_i\rangle\right|^2}{\omega/\hbar+(E_0-E_i)/\hbar+i\eta} + \sum_i \frac{\left|\langle\Psi_0|c_{\mu m_\mu}^{\dagger}|\Psi_i\rangle\right|^2}{\omega/\hbar+(E_i-E_0)/\hbar-i\eta} \ , \qquad (112)\\
G_{\mu}^{22}(\omega) &\stackrel{d}{=} \lim_{\eta\to+0}\int_{-\infty}^{\infty} dt\, e^{i\omega t/\hbar}\, G_{\mu}^{22}(t)\, e^{-(2\theta(t)-1)\eta t} \\
&= \sum_i \frac{\left|\langle\Psi_0|c_{\overline{\mu m_\mu}}^{\dagger}|\Psi_i\rangle\right|^2}{\omega/\hbar+(E_0-E_i)/\hbar+i\eta} + \sum_i \frac{\left|\langle\Psi_0|c_{\overline{\mu m_\mu}}|\Psi_i\rangle\right|^2}{\omega/\hbar+(E_i-E_0)/\hbar-i\eta} \ . \qquad (113)
\end{aligned}
$$

Thus it is seen that we can put

$$
\begin{aligned}
\frac{1}{\hbar}G_{\mu}^{11}(\omega) &= \sum_a\left(\frac{R_{\mu a}^{11}(\omega_{G+}^{\mu a})}{\omega-\omega_{G+}^{\mu a}} + \frac{R_{\mu a}^{11}(-\omega_{G+}^{\mu a})}{\omega+\omega_{G+}^{\mu a}}\right)e^{i\omega\eta} \ , \qquad (114)\\
\frac{1}{\hbar}G_{\mu}^{22}(\omega) &= \sum_a\left(\frac{R_{\mu a}^{22}(\omega_{G+}^{\mu a})}{\omega-\omega_{G+}^{\mu a}} + \frac{R_{\mu a}^{22}(-\omega_{G+}^{\mu a})}{\omega+\omega_{G+}^{\mu a}}\right)e^{-i\omega\eta} \ . \qquad (115)
\end{aligned}
$$

The factor $e^{i\omega\eta}$ ($e^{-i\omega\eta}$) in $G_{\mu}^{11}(\omega)$ ($G_{\mu}^{22}(\omega)$) comes from the definition of the Green functions at $t=0$:

$$
\begin{aligned}
G_{\mu}^{11}(t=0) &= \lim_{t\to-0} G_{\mu}^{11}(t) \ , \qquad (116)\\
G_{\mu}^{22}(t=0) &= \lim_{t\to+0} G_{\mu}^{22}(t) \ . \qquad (117)
\end{aligned}
$$

See section 7-2 in [43]. From the time-reversal invariance it follows that

$$
\begin{aligned}
E_i &= E_{\overline{i}} \ , \qquad (118)\\
\hat{T}|\Psi_0\rangle &= \hat{T}^{-1}|\Psi_0\rangle = |\Psi_0\rangle \ , \qquad (119)\\
\{|\Psi_i\rangle\}_{i=\cdots} &= \{|\Psi_{\overline{i}}\rangle\}_{\overline{i}=\cdots} \ , \qquad (120)
\end{aligned}
$$

where $\hat{T}$ is the time-reversal operator. In addition we have

$$\hat{T}^{-1}|\Psi_i\rangle = -\hat{T}|\Psi_i\rangle = -|\Psi_{\overline{i}}\rangle \ . \tag{121}$$

The negative sign is due to that $|\Psi_i\rangle$ is an odd particle-number state. By using Eqs. (118) – (121), Eq. (113) becomes

$$\begin{aligned} G^{22}_{\mu}(\omega) &= \sum_i \frac{\left|\langle \hat{T}^{-1}\Psi_0|c^{\dagger}_{\mu m_\mu}\hat{T}^{-1}|\Psi_i\rangle\right|^2}{\omega/\hbar + (E_0 - E_i)/\hbar + i\eta} + \sum_i \frac{\left|\langle \hat{T}^{-1}\Psi_0|c_{\mu m_\mu}\hat{T}^{-1}|\Psi_i\rangle\right|^2}{\omega/\hbar + (E_i - E_0)/\hbar - i\eta} \\ &= \sum_i \frac{\left|\langle \Psi_0|c^{\dagger}_{\mu m_\mu}|\Psi_i\rangle\right|^2}{\omega/\hbar + (E_0 - E_i)/\hbar + i\eta} + \sum_i \frac{\left|\langle \Psi_0|c_{\mu m_\mu}|\Psi_i\rangle\right|^2}{\omega/\hbar + (E_i - E_0)/\hbar - i\eta} \ . \end{aligned} \tag{122}$$

This equation implies

$$G^{22}_{\mu}(-\omega) = -G^{11}_{\mu}(\omega) \ . \tag{123}$$

For the residues we have the relations

$$R^{22}_{\mu a}(\omega^{\mu a}_{G+}) = R^{11}_{\mu a}(-\omega^{\mu a}_{G+}) \ , \tag{124}$$

$$R^{22}_{\mu a}(-\omega^{\mu a}_{G+}) = R^{11}_{\mu a}(\omega^{\mu a}_{G+}) \ . \tag{125}$$

The anomalous Green functions are defined as

$$G^{12}_{\mu}(t) = -i\langle \Psi_0|\mathrm{T}[c_{\mu m_\mu}(t)c_{\overline{\mu m_\mu}}]|\Psi_0\rangle \ , \tag{126}$$

$$G^{21}_{\mu}(t) = -i\langle \Psi_0|\mathrm{T}[c^{\dagger}_{\overline{\mu m_\mu}}(t)c^{\dagger}_{\mu m_\mu}]|\Psi_0\rangle \ . \tag{127}$$

In the same manner as discussed for $G^{11}_{\mu}(\omega)$ and $G^{22}_{\mu}(\omega)$, it turns out that

$$G^{12}_{\mu}(\omega) = \sum_i \frac{\langle \Psi_0|c_{\mu m_\mu}|\Psi_i\rangle\langle \Psi_i|c_{\overline{\mu m_\mu}}|\Psi_0\rangle}{\omega/\hbar + (E_0 - E_i)/\hbar + i\eta} - \sum_i \frac{\langle \Psi_0|c_{\mu m_\mu}|\Psi_i\rangle^*\langle \Psi_i|c_{\overline{\mu m_\mu}}|\Psi_0\rangle^*}{\omega/\hbar + (E_i - E_0)/\hbar - i\eta} \ , \tag{128}$$

$$G^{21}_{\mu}(\omega) = \sum_i \frac{\langle \Psi_0|c^{\dagger}_{\overline{\mu m_\mu}}|\Psi_i\rangle\langle \Psi_i|c^{\dagger}_{\mu m_\mu}|\Psi_0\rangle}{\omega/\hbar + (E_0 - E_i)/\hbar + i\eta} - \sum_i \frac{\langle \Psi_0|c^{\dagger}_{\overline{\mu m_\mu}}|\Psi_i\rangle^*\langle \Psi_i|c^{\dagger}_{\mu m_\mu}|\Psi_0\rangle^*}{\omega/\hbar + (E_i - E_0)/\hbar - i\eta} \ . \tag{129}$$

Thus one can put

$$\frac{1}{\hbar}G^{12}_{\mu}(\omega) = \sum_a \left(\frac{R^{12}_{\mu a}(\omega^{\mu a}_{G+})}{\omega - \omega^{\mu a}_{G+}} + \frac{R^{12}_{\mu a}(-\omega^{\mu a}_{G+})}{\omega + \omega^{\mu a}_{G+}} \right) \ , \tag{130}$$

$$\frac{1}{\hbar}G^{21}_{\mu}(\omega) = \sum_a \left(\frac{R^{21}_{\mu a}(\omega^{\mu a}_{G+})}{\omega - \omega^{\mu a}_{G+}} + \frac{R^{21}_{\mu a}(-\omega^{\mu a}_{G+})}{\omega + \omega^{\mu a}_{G+}} \right) \ , \tag{131}$$

with the relations

$$R^{12}_{\mu a}(-\omega^{\mu a}_{G+}) = -R^{12\,*}_{\mu a}(\omega^{\mu a}_{G+}) \ , \tag{132}$$

$$R^{21}_{\mu a}(-\omega^{\mu a}_{G+}) = -R^{21\,*}_{\mu a}(\omega^{\mu a}_{G+}) \ , \tag{133}$$

$$R^{21}_{\mu a}(\omega^{\mu a}_{G+}) = -R^{12}_{\mu a}(-\omega^{\mu a}_{G+}) = R^{12\,*}_{\mu a}(\omega^{\mu a}_{G+}) \ , \tag{134}$$

$$R^{21}_{\mu a}(-\omega^{\mu a}_{G+}) = -R^{12}_{\mu a}(\omega^{\mu a}_{G+}) = R^{12\,*}_{\mu a}(-\omega^{\mu a}_{G+}) \ . \tag{135}$$

It is worthy to note that a relation holds regardless of the time-reversal invariance of $|\Psi_0\rangle$:

$$R^{11}_{\mu a}(\omega^{\mu a}_{G+})R^{22}_{\mu a}(\omega^{\mu a}_{G+}) = \left|R^{12}_{\mu a}(\omega^{\mu a}_{G+})\right|^2 \ . \tag{136}$$

Let us assume that the energy of $|\Psi_i\rangle$ is equal to that of $|\Psi_{i'}\rangle$ with a different particle number incidentally. Then we can introduce the basis state $|\Psi_i\rangle$ which has a mixed particle number. In this way it is possible that $R^{11}_{\mu a}(\omega^{\mu a}_{G+})$ and $R^{11}_{\mu a}(-\omega^{\mu a}_{G+})$ are non-zero simultaneously without causing a problem, if the system is ideally large.

Appendix D – formula of pole and residue –

As is mentioned in the text, we determine the real part of the pole of the perturbed nucleon Green function approximately by the condition

$$\det \overline{G}^{-1}_{\mu}(\pm \mathrm{Re}\,\omega^{\mu a}_{G+}) = 0 \ , \tag{137}$$

where $\overline{G}^{-1}_{\mu}(\omega)$ is a matrix in which the non-hermitian components of $G^{-1}_{\mu}(\omega)$ were eliminated. The advantage of this method is that the pole search is a one-dimensional problem.

Using Eq. (12) in the text, we obtain

$$\left(\frac{d}{d\omega}\frac{\hbar}{G^{11}_{\mu}(\omega)}\right)^{-1} = -\frac{\left\{\sum_a \left(\frac{R^{11}_{\mu a}(\omega^{\mu a}_{G+})}{\omega-\omega^{\mu a}_{G+}} + \frac{R^{11}_{\mu a}(-\omega^{\mu a}_{G+})}{\omega+\omega^{\mu a}_{G+}}\right)\right\}^2}{\sum_a \left(-\frac{R^{11}_{\mu a}(\omega^{\mu a}_{G+})}{(\omega-\omega^{\mu a}_{G+})^2} - \frac{R^{11}_{\mu a}(-\omega^{\mu a}_{G+})}{(\omega+\omega^{\mu a}_{G+})^2}\right)} \ . \tag{138}$$

Therefore it is found that

$$\lim_{\omega\to\pm\omega^{\mu a}_{G+}} \left(\frac{d}{d\omega}\frac{\hbar}{G^{11}_{\mu}(\omega)}\right)^{-1} = R^{11}_{\mu a}(\pm\omega^{\mu a}_{G+}) \ , \tag{139}$$

and in accordance with Eq. (137) we approximate

$$R^{11}_{\mu a}(\pm\omega^{\mu a}_{G+}) \simeq \lim_{\omega\to\pm\mathrm{Re}\,\omega^{\mu a}_{G+}} \left(\frac{d}{d\omega}\frac{\hbar}{\overline{G}^{11}_{\mu}(\omega)}\right)^{-1} \ . \tag{140}$$

The following equation may be more convenient in the numerical calculation:

$$R^{11}_{\mu a}(\pm\omega^{\mu a}_{G+}) \simeq \left.\frac{\omega+\varepsilon^0_\mu-\varepsilon_F-\hbar\overline{\Sigma}^{22}_{\mu}(\omega)}{\frac{d}{d\omega}\hbar^2\det\overline{G}^{-1}_{\mu}(\omega)}\right|_{\omega=\pm\mathrm{Re}\,\omega^{\mu a}_{G+}} \ , \tag{141}$$

where $\overline{\Sigma}_{\mu}(\omega)$ is defined in the same way as $\overline{G}_{\mu}{}^{-1}$.

For the pairing part we have

$$\begin{aligned} R^{12}_{\mu a}(\pm\omega^{\mu a}_{G+}) &\simeq \lim_{\omega\to\pm\mathrm{Re}\,\omega^{\mu a}_{G+}} \left(\frac{d}{d\omega}\frac{\hbar}{\overline{G}^{12}_{\mu}(\omega)}\right)^{-1} \\ &= \left.\frac{\overline{\Sigma}^{12}_{\mu}(\omega)}{\frac{d}{d\omega}\hbar\det\overline{G}^{-1}_{\mu}(\omega)}\right|_{\omega=\pm\mathrm{Re}\,\omega^{\mu a}_{G+}} \ . \end{aligned} \tag{142}$$

For the imaginary part of the pole it is derived that

$$\begin{aligned}\mathrm{Im}\frac{\hbar}{G^{11}_{\mu}(\pm\mathrm{Re}\,\omega^{\mu a}_{G+})}R^{11}_{\mu a}(\pm\omega^{\mu a}_{G+}) &= \mathrm{Im}\frac{R^{11}_{\mu a}(\pm\omega^{\mu a}_{G+})}{\sum_{a'}\left(\frac{R^{11}_{\mu a}(\omega^{\mu a'}_{G+})}{\pm\mathrm{Re}\,\omega^{\mu a}_{G+}-\omega^{\mu a'}_{G+}}+\frac{R^{11}_{\mu a}(-\omega^{\mu a'}_{G+})}{\pm\mathrm{Re}\,\omega^{\mu a}_{G+}+\omega^{\mu a'}_{G+}}\right)} \\ &\simeq \mp\mathrm{Im}\,\omega^{\mu a}_{G+}\ . \end{aligned} \tag{143}$$

This approximation is based on a condition that the imaginary part of the pole is very small.

Appendix E – total energy –

Derivation of the equation of the total energy is possible in the same way as that for the case without the pairing. (See sections 7 (Chap.3) and 46 (Chap.12) in [62]). We put the Hamiltonian

$$\begin{aligned} H &= \sum_{\mu m_\mu}\tilde{\varepsilon}^0_{\mu}c^{\dagger}_{\mu m_\mu}c_{\mu m_\mu}+\varepsilon_F\langle\hat{N}\rangle \\ &\quad+\sum_{\lambda m}\hat{\alpha}_{\lambda m}\sum_{\mu m_\mu\nu m_\nu}\langle\mu m_\mu|\kappa_\lambda F^{\dagger}_{\lambda m}|\nu m_\nu\rangle c^{\dagger}_{\mu m_\mu}c_{\nu m_\nu} \\ &\quad+\sum_{\lambda m}\hbar\Omega_\lambda(c^{\dagger}_{\lambda m}c_{\lambda m}+\frac{1}{2})\ . \end{aligned} \tag{144}$$

The expectation value of the particle number $\langle\hat{N}\rangle$ was taken in advance. For the particle-phonon coupling, see Appendix A. $\hbar\Omega_\lambda$ is the phonon energy. We consider

$$c_{\mu m_\mu}(t)=e^{iHt/\hbar}c_{\mu m_\mu}e^{-iHt/\hbar}\ , \tag{145}$$

$$\hat{\alpha}_{\lambda m}(t)=e^{iHt/\hbar}\hat{\alpha}_{\lambda m}e^{-iHt/\hbar}\ . \tag{146}$$

Then it follows that

$$i\hbar\frac{\partial}{\partial t}c_{\mu m_\mu}(t)=\tilde{\varepsilon}^0_{\mu}c_{\mu m_\mu}(t)+\sum_{\lambda m}\hat{\alpha}_{\lambda m}(t)\sum_{\nu m_\nu}\langle\mu m_\mu|\kappa_\lambda F^{\dagger}_{\lambda m}|\nu m_\nu\rangle c_{\nu m_\nu}(t)\ . \tag{147}$$

Multiplying $c^{\dagger}_{\mu m_\mu}(t')$, $t'>t$, from the left, using the definition of the particle Green function in the time representation and putting $t=0$, one finds

$$\begin{aligned}&\lim_{t'\to+0}\left(i\hbar\frac{\partial}{\partial t}\sum_{\mu m_\mu}(-i)G^{11}_{\mu}(t,t')\Big|_{t=0}\right) \\ &\quad=\langle\sum_{\mu m_\mu}\tilde{\varepsilon}^0_{\mu}c^{\dagger}_{\mu m_\mu}c_{\mu m_\mu}\rangle+\left\langle\sum_{\lambda m}\hat{\alpha}_{\lambda m}\sum_{\mu m_\mu\nu m_\nu}\langle\mu m_\mu|\kappa_\mu F^{\dagger}_{\lambda m}|\nu m_\nu\rangle c^{\dagger}_{\mu m_\mu}c_{\nu m_\nu}\right\rangle\ . \end{aligned} \tag{148}$$

By using the Green function in Lehmann representation, it turns out that

$$\begin{aligned}\langle H\rangle &= -i\lim_{\eta\to+0}\sum_{\mu m_\mu}\int_{-\infty}^{\infty}\frac{d\omega}{2\pi}\frac{1}{\hbar}\omega G^{11}_{\mu}(\omega)e^{i\omega\eta}+\varepsilon_F\langle\hat{N}\rangle+\langle\sum_{\lambda m}\hbar\Omega_\lambda(c^{\dagger}_{\lambda m}c_{\lambda m}+1/2)\rangle \\ &= \sum_{\mu m_\mu}\sum_{a}(-\omega^{\mu a}_{G+})R^{11}_{\mu a}(-\omega^{\mu a}_{G+})+\varepsilon_F\langle\hat{N}\rangle+\langle H^{\mathrm{ph}}_0\rangle\ , \end{aligned} \tag{149}$$

where $H_0^{\rm ph}$ denotes the fourth term in Eq. (144). ω in our notation always indicates energy. The last equation is derived for the ground state, for which the poles with positive infinitesimal imaginary part have negative real part. ($\mathrm{Re}\,\omega_{G+}^{\mu a} > 0$)

It is possible to rewrite the total energy by using Dyson equation as follows:

$$
\begin{aligned}
&\langle H\rangle - \langle H_0^{\rm ph}\rangle \\
&= \varepsilon_F\langle\hat{N}\rangle - i\sum_{\mu m_\mu}\frac{1}{2}\lim_{\eta\to+0}\int_{-\infty}^{\infty}\frac{d\omega}{2\pi}\mathrm{Tr}\left[\begin{pmatrix}\omega & 0\\ 0 & \omega\end{pmatrix}\frac{1}{\hbar}G_\mu(\omega)\begin{pmatrix}e^{i\eta\omega} & 0\\ 0 & e^{-i\eta\omega}\end{pmatrix}\right] \\
&= \varepsilon_F\langle\hat{N}\rangle - i\sum_{\mu m_\mu}\frac{1}{2}\lim_{\eta\to+0}\int_{-\infty}^{\infty}\frac{d\omega}{2\pi}\mathrm{Tr}\left[\left\{\hbar G_\mu^{-1}(\omega)\right.\right. \\
&\quad \left.\left. + \begin{pmatrix}\tilde{\varepsilon}_\mu^0 & 0\\ 0 & -\tilde{\varepsilon}_\mu^0\end{pmatrix} + \hbar\Sigma_\mu(\omega)\right\}\frac{1}{\hbar}G_\mu(\omega)\begin{pmatrix}e^{i\eta\omega} & 0\\ 0 & e^{-i\eta\omega}\end{pmatrix}\right] \\
&= \sum_{\mu m_\mu}\sum_a \varepsilon_\mu^0 R_{\mu a}^{11}(-\omega_{G+}^{\mu a}) - i\sum_{\mu m_\mu}\frac{1}{2}\lim_{\eta\to+0}\int_{-\infty}^{\infty}\frac{d\omega}{2\pi}\left(\hbar\Sigma_\mu^{11}(\omega)\frac{1}{\hbar}G_\mu^{11}(\omega)e^{i\eta\omega}\right. \\
&\quad +\hbar\Sigma_\mu^{12}(\omega)\frac{1}{\hbar}G_\mu^{21}(\omega)e^{i\eta\omega} + \hbar\Sigma_\mu^{21}(\omega)\frac{1}{\hbar}G_\mu^{12}(\omega)e^{-i\eta\omega} \\
&\quad \left.+\hbar\Sigma_\mu^{22}(\omega)\frac{1}{\hbar}G_\mu^{22}(\omega)e^{-i\eta\omega}\right)\ , \qquad (150)
\end{aligned}
$$

We have used the relation between $G_\mu^{11}(\omega)$ and $G_\mu^{22}(\omega)$ (Appendix C). A reasonable definition of the pairing energy may be

$$
E_{\rm pair} = -i\sum_{\mu m_\mu}\frac{1}{2}\lim_{\eta\to+0}\int_{-\infty}^{\infty}\frac{d\omega}{2\pi}\left(\hbar\Sigma_\mu^{12}(\omega)\frac{1}{\hbar}G_\mu^{21}(\omega)e^{i\eta\omega} + \hbar\Sigma_\mu^{21}(\omega)\frac{1}{\hbar}G_\mu^{12}(\omega)e^{-i\eta\omega}\right)\ . \qquad (151)
$$

A factor $i/2$ is necessary in the diagramatic derivation. If one puts $\hbar\Sigma_\mu^{12}(\omega) \simeq \hbar\Sigma_\mu^{12}(\omega_{G+}^{\mu a_0})$ in addition to the conditions which are used for deriving Eq. (49), then we have

$$
E_{\rm pair} \simeq \sum_\mu (2j_\mu+1)u_\mu v_\mu \Delta_\mu\ . \qquad (152)
$$

It is noted that Eq. (152) differs from the known pairing energy in the BCS approximation by a factor 2. This is because the particle-phonon interaction introduced in our calculation is not of the two-body type (see Eq. (54), [62] and its chap. 12).

Appendix F – pairing gap –

The equation to determine the pole is given by

$$
\begin{aligned}
0 &= \hbar^2 \mathrm{Re}\,\det G_\mu^{-1}(\mathrm{Re}\,\omega_{G+}^{\mu a}) \\
&= \begin{vmatrix} \mathrm{Re}\,\omega_{G+}^{\mu a} - \tilde{\varepsilon}_\mu^0 - \mathrm{Re}\,\hbar\Sigma_\mu^{11}(\mathrm{Re}\,\omega_{G+}^{\mu a}) & -\hbar\Sigma_\mu^{12}(\mathrm{Re}\,\omega_{G+}^{\mu a}) \\ -\hbar\Sigma_\mu^{21}(\mathrm{Re}\,\omega_{G+}^{\mu a}) & \mathrm{Re}\,\omega_{G+}^{\mu a} + \tilde{\varepsilon}_\mu^0 - \mathrm{Re}\,\hbar\Sigma_\mu^{22}(\mathrm{Re}\,\omega_{G+}^{\mu a}) \end{vmatrix}\ . \qquad (153)
\end{aligned}
$$

We define functions

$$
Z_\mu(\omega_{G+}^{\mu a}) \stackrel{d}{=} 1 - \frac{1}{\omega_{G+}^{\mu a}}\mathrm{Re}\,\hbar\Sigma_\mu^{11\,\rm odd}(\omega_{G+}^{\mu a})\ , \qquad (154)
$$

$$\Sigma_\mu^{11\,\mathrm{odd}}(\omega_{G+}^{\mu a}) \stackrel{d}{=} \frac{1}{2}\left(\Sigma_\mu^{11}(\omega_{G+}^{\mu a}) - \Sigma_\mu^{11}(-\omega_{G+}^{\mu a})\right) \ , \tag{155}$$

$$\Sigma_\mu^{11\,\mathrm{even}}(\omega_{G+}^{\mu a}) \stackrel{d}{=} \frac{1}{2}\left(\Sigma_\mu^{11}(\omega_{G+}^{\mu a}) + \Sigma_\mu^{11}(-\omega_{G+}^{\mu a})\right) \ . \tag{156}$$

By dividing by $(\ Z_\mu(\mathrm{Re}\,\omega_{G+}^{\mu a})\ )^2$, Eq. (153) can be written

$$0 = \left| \begin{array}{cc} \mathrm{Re}\,\omega_{G+}^{\mu a} - \frac{\tilde{\varepsilon}_\mu^0 + \mathrm{Re}\,\hbar\Sigma_\mu^{11\,\mathrm{even}}(\mathrm{Re}\,\omega_{G+}^{\mu a})}{Z_\mu(\mathrm{Re}\,\omega_{G+}^{\mu a})} & -\frac{\hbar\Sigma_\mu^{12}(\mathrm{Re}\,\omega_{G+}^{\mu a})}{Z_\mu(\mathrm{Re}\,\omega_{G+}^{\mu a})} \\ -\frac{\hbar\Sigma_\mu^{21}(\mathrm{Re}\,\omega_{G+}^{\mu a})}{Z_\mu(\mathrm{Re}\,\omega_{G+}^{\mu a})} & \mathrm{Re}\,\omega_{G+}^{\mu a} + \frac{\tilde{\varepsilon}_\mu^0 + \mathrm{Re}\,\hbar\Sigma_\mu^{11\,\mathrm{even}}(\mathrm{Re}\,\omega_{G+}^{\mu a})}{Z_\mu(\mathrm{Re}\,\omega_{G+}^{\mu a})} \end{array} \right| \ . \tag{157}$$

We have used $\Sigma_\mu^{22}(\omega) = -\Sigma_\mu^{11}(-\omega)$. The diagonal elements of Eq. (157) has the structure of the BCS equation for a time-reversal-invariant state. Therefore it is usual to define the pairing gap by

$$\Delta_\mu = \frac{\hbar\Sigma_\mu^{12}(\mathrm{Re}\,\omega_{G+}^{\mu a_0})}{Z_\mu(\mathrm{Re}\,\omega_{G+}^{\mu a_0})} \ . \tag{158}$$

(See sections 7-2 in [43], 10 in [44] and [47].) a_0 in Eq. (158) indicates the quasiparticle pole. From Eq. (157) it is also seen that

$$Z_\mu(\mathrm{Re}\,\omega_{G+}^{\mu a_0}) = \frac{1}{\mathrm{Re}\,\omega_{G+}^{\mu a_0}}\sqrt{(\ \tilde{\varepsilon}_\mu^0 + \mathrm{Re}\,\hbar\Sigma_\mu^{11\,\mathrm{even}}(\mathrm{Re}\,\omega_{G+}^{\mu a_0})\ )^2 + \left|\hbar\Sigma_\mu^{12}(\mathrm{Re}\,\omega_{G+}^{\mu a_0})\right|^2} \ . \tag{159}$$

In the same way the perturbed single-particle energy is given by

$$\tilde{\varepsilon}_\mu^1 = \frac{1}{Z_\mu(\mathrm{Re}\,\omega_{G+}^{\mu a_0})}(\ \tilde{\varepsilon}_\mu^0 + \mathrm{Re}\,\hbar\Sigma_\mu^{11\,\mathrm{even}}(\mathrm{Re}\,\omega_{G+}^{\mu a_0})\ ) \ . \tag{160}$$

References

[1] A. Bohr, B. R. Mottelson and D. Pines, *Phys. Rev.* **110** (1958) 936

[2] A. Bohr, B. R. Mottelson, "Nuclear Structure", Vol.I, W.A.Benjamin, New York, 1969

[3] A. Bohr, B. R. Mottelson, "Nuclear Structure", Vol.II, W.A.Benjamin, Reading,Massachusetts, 1975

[4] R. A. Broglia, O. Hansen and C. Riedel, *in* "Adv. in Nucl. Phys." (M. Baranger and E. Vogt, Eds.), Vol. 6, p.287, Plenum press., New York, 1973

[5] H. J. Mang and J. O. Rasmussen, *Mat. Fys. Skr. Dan Vid. Selsk.* **2** no.3

[6] O. Nathan and S. G. Nilsson, *in* "Alpha-, Beta- and Gamma-Ray Spectroscopy" (K. Siegbahn, Ed.), chapter 10, North-Holland, Amsterdam, 1965

[7] B. R. Mottelson and J. G. Valatin, *Phys. Rev. Lett.* **5** (1960) 511

[8] R. A. Sorensen, *Rev. Mod. Phys.* **45** (1973) 353

[9] D. R. Bes and R. A. Sorensen, *in* "Adv. in Nucl. Phys." (M. Baranger and E. Vogt, Eds.), Vol. 2, p.129, Plenum press, New York, 1969

[10] M. Wakai and A. Faessler, *Nucl. Phys. A* **295** (1978) 86

[11] D. R. Bes and R. A. Broglia, *Phys. Rev. C* **3** (1971) 2349

[12] L. S. Kisslinger and R. A. Sorensen, *Rev. Mod. Phys.* **35** (1963) 853

[13] A. Plastino, R. Arvieu and S. A. Moszkowski, *Phys. Rev.* **145** (1966) 837

[14] A. Faessler and A. Plastino, *Nucl. Phys. A* **94** (1967) 580

[15] G. F. Bertsch and H. Esbensen, *Ann. Phys. (N.Y.)* **209** (1991) 327

[16] D. Gogny, *Nucl. Phys. A* **237** (1975) 399

[17] J. Dechargé and D. Gogny, *Phys. Rev. C* **21** (1980) 1568

[18] J. Dobaczewski, W. Nazarewicz, T.R. Werner, J.F. Berger, C.R. Chinn and J. Dechargé *Phys. Rev. C* **53** (1996) 2809

[19] J. Terasaki, P.-H. Heenen, H. Flocard and P. Bonche, *Nucl. Phys. A* **600** (1996) 371

[20] D.S. Delion, M. Baldo and U. Lombardo, *Nucl. Phys. A* **593** (1995) 151

[21] F. Barranco, R.A. Broglia, H.Esbensen and E. Vigezzi, *Phys. Lett. C* **390** (1996) 13

[22] A. L. Goodman, *in* "Adv. in Nucl. Phys." Vol. 11, p.263, Plenum press, New York, 1979

[23] L. Amundsen and E. Østgaard, *Nucl. Phys. A* **437** (1985) 487

[24] M. Baldo, J. Cugnon, A. Lejeune and U. Lombardo, *Nucl. Phys. A* **515** (1990) 409

[25] T. Takatsuka and R. Tamagaki, *Prog. Theor. Phys. Suppl.* **112** (1993) 27

[26] U. Lombardo, H.-J. Schulze and W. Zuo, *Phys. Lett. B* **59** (1999) 2927

[27] U. Lombardo, *in* "Nuclear Methods and the Nuclear Equation of State" (M. Baldo, Ed.), World Scientific, Singapore, 1999

[28] L. B. Leinson, *Phys. Lett. B* **473** (2000) 318

[29] S. Babu and G.E. Brown, *Ann. Phys. (N.Y.)* **78** (1973) 1

[30] V. Bernard and N.V. Giai, *Nucl. Phys. A* **348** (1980) 75

[31] J.M.C. Chen, J.W. Clark, R.D. Davé and V.V. Khodel, *Nucl. Phys. A* **555** (1993) 59

[32] J. Wambach, T.L. Ainsworth and D. Pines, *Nucl. Phys. A* **555** (1993) 128

[33] P. Bożek, *Nucl. Phys. A* **657** (1999) 187

[34] M. Baldo and A. Grasso, *Phys. Lett. B* **485** (2000) 115

[35] C. Mahaux, P. F. Bortignon, R. A. Broglia and C. H. Dasso, *Phys. Rep.* **120** (1985) 1.

[36] S. T. Belyaev, *Sov. Phys. JETP* **12** (1961) 968

[37] S. T. Belyaev and V. G. Zelevinskii, *Sov. J. Nucl. Phys.* **2** (1966) 35

[38] S. T. Belyaev, *Sov. J. Nucl. Phys.* **1** (1965) 3

[39] A. B. Migdal, "Theory of Finite Fermi Systems and Application to Atomic Nuclei", Interscience pub., New York, 1967

[40] A. B. Migdal, "Nuclear Theory: The Quasiparticle Method", W. A. Benjamin, Inc., New York, 1968

[41] L. P. Gor'kov, *Sov. Phys. JETP* **7** (1958) 505

[42] Y. Nambu, *Phys. Rev.* **117** (1960) 648

[43] J. R. Schrieffer, "Theory of Superconductivity", chapter 7, Addison-Wesley, Redwood City, 1964

[44] P. B. Allen and B. Mitrović, *in* "Solid State Physics" (H. Ehrenreich, F. Seitz and D. Turnbull, Eds.), Vol.37, p. 1 Academic press, New York, 1982

[45] F. Barranco et al, *Phys. Rev. Lett.* **83** (1999) 2147

[46] F. Barranco, P. F. Bortignon, R. A. Broglia, G. Colò and E. Vigezzi, *Eur. Phys. J. A* **11** (2001).

[47] A. V. Avdeenkov and S. P. Kamerdzhiev, *Phys. Atom. Nucl.* **62** (1999) 563

[48] S. G. Kadmenskii, P. A. Lukyanovich, Yu. I. Remesov and V. I. Furman, *Sov. J. Nucl. Phys.* **45** (1987) 585

[49] H. Müther, T. Taigel and T. T. S. Kuo, *Nucl. Phys. A* **482** (1988) 601

[50] W. H. Dickhoff and H. Müther, *Rep. Prog. Phys.* **11** (1992) 1947

[51] H. Müther and L. D. Skouras, *Nucl. Phys. A* **555** (1993) 541

[52] H. Müther and L. D. Skouras, *Phys. Lett. B* **306** (1993) 201

[53] H. Müther and L. D. Skouras, *Nucl. Phys. A* **581** (1995) 247

[54] K. Amir-Azimi-Nili, H. Müther, L. D. Skouras and A. Polls, *Nucl. Phys. A* **604** (1996) 245

[55] B. E. Vonderfecht, C. C. Gearhart and W. H. Dickhoff, *Phys. Lett. B* **253** (1991) 1

[56] D. Van Neck, M. Waroquier and J. Ryckebusch, *Phys. Lett. B* **249** (1990) 157

[57] D. Van Neck, M. Waroquier and J. Ryckebusch, *Nucl. Phys. A* **530** (1991) 347

[58] D. Van Neck, M. Waroquier, V. Van der Sluys and K. Heyde, *Nucl. Phys. A* **563** (1993) 1

[59] V. Van der Sluys, D. Van Neck, M. Waroquier and J. Ryckebusch, *Nucl. Phys. A* **551** (1993) 210

[60] Y. Dewulf, D. Van Neck, L. Van Daele and M. Waroquier, *Phys. Lett. B* **396** (1997) 7

[61] A.A. Abrikosov, L.P. Gorkov and I.E. Dzyaloshinski, "Methods of Quantum Field Theory in Statistical Physics", Dover, New York, 1975

[62] A. L. Fetter and J. .D. Walecka, "Quantum Theory of Many-Particle Systems", chapter 3, McGraw-Hill, New York, 1971

[63] F.J. Eckle et al., *Nucl. Phys. A* **506** (1990) 159

[64] J. Terasaki, F. Barranco, R. A. Broglia, E. Vigezzi and P. F. Bortignon, to be published in *Nucl. Phys. A*